

MODELING CLIMATE CHANGE IMPACTS ON FLOODING
AND COMMUNITY VULNERABILITY
NOVATO, CA

AS
36
2019
ERTH
.G65

A thesis submitted to the faculty of
San Francisco State University
In partial fulfillment of
the requirements for
the Degree

Master of Science

In

Geoscience

by

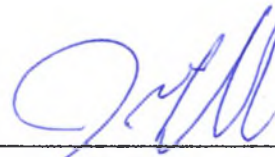
Suzanne D. Goldstein

San Francisco, California

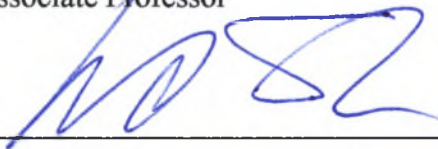
May 2019

CERTIFICATION OF APPROVAL

I certify that I have read Modeling Climate Change Impacts on Flooding and Community Vulnerability, Novato, CA by Suzanne D. Goldstein, and that in my opinion this work meets the criteria for approving a thesis submitted in partial fulfillment of the requirement for the degree Master of Science in Geoscience at San Francisco State University.



Jason J. Gurdak, Ph.D.
Associate Professor



Leonard S. Sklar, Ph.D.
Emeritus



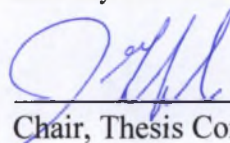
Edwin P. Maurer, Ph.D.
Professor
Santa Clara University

MODELING CLIMATE CHANGE IMPACTS ON FLOODING
AND COMMUNITY VULNERABILITY
NOVATO, CA

Suzanne D. Goldstein
San Francisco, California
2019

This study investigates the effects of climate change on compound fluvial and coastal flooding using coupled hydrologic and hydraulic models to examine the changing physical characteristics and socio-economic impacts of flooding in a small basin typical of many flood-prone areas on the United States west coast. Novato Creek is located in Marin County, California along the northeastern edge of San Francisco Bay. With steep, densely populated communities upstream and major regional transportation and utility infrastructure in low-lying areas near the bay, the watershed is highly vulnerable to climate change. Downscaled daily precipitation projections from an ensemble of 10 Global Climate Models indicate that the magnitude of a two-day, 50-year (2% annual chance of occurrence) storm will increase by an average of $16\% \pm 6\%$ by mid-century (2040-69) and $31\% \pm 8\%$ by late-century (2070-99) under a high emissions (RCP 8.5) trajectory. These increases in precipitation, combined with sea level rise (SLR) projections of 0.6 to 1 m (1.9 to 3.4 ft) by mid-century and 1.0 to 1.9 m (3.4 to 5.2 ft) by late-century, will lead to median increases in flood extent of 42% to 77% by mid-century and 82% to 83% by late-century. Socio-economic impacts from this compound flooding are significantly greater than the impacts of SLR or changing precipitation alone. The total number of people impacted by flooding will increase from 6,500 under historic storm conditions to at least 9,400 by mid-century and 11,400 by late-century. The length of roads impacted by flooding will increase 60% to 170%, and as many as 2,400 to 3,250 homes and other buildings will be exposed to flooding. The scale of these projected impacts makes clear the importance of considering compound flood effects when planning for climate change adaptation.

I certify that the abstract is a correct representation of the content of this thesis.



Chair, Thesis Committee

5-21-2019
Date

ACKNOWLEDGEMENTS

I am grateful to many people for their support, encouragement, and patience through the long and winding process of completing this thesis and my broader journey into a career in geoscience. This project could not have happened without the early leadership of Dr. Leonard S. Sklar and his shared vision for my graduate school quest, together with the steady coaching and guidance of my Committee Chair Dr. Jason J. Gurdak. I am also very grateful that Dr. Edwin P. Maurer lent his expertise to this project, always warmly giving his time and attention. I am indebted to Roger Leventhal of the Marin County Department of Public Works (DPW) who facilitated funding for this work and provided many hours of help and feedback, as well as developed the original HEC-HMS hydrologic model underlying the entire project. Additionally, I would like to thank Melissa Reardon and Alexandra Oran of Schaaf & Wheeler Consulting who developed the HEC-RAS hydraulic model and patiently responded to my many questions.

Above all else, I wish to thank the family and friends who have sustained me throughout this endeavor. I am immeasurably grateful to my parents whose confidence in me has never wavered and whose constant love and support is the bedrock on which all of my accomplishments stand. I also could not have done this without the many friends who cheered me on, including a special few – Tom Steinbach, Sarah Abbe Taylor, Richard Gross, Donovan Fones, Gloria Beck, Fiona Shinkfield, Amy Luckey, Julie Ford, Kimmy Carter, Sharon Knight – whose kindness and generosity made all the difference.

Finally, I would like to thank the Achievement Rewards for College Scientists (ARCS) Foundation, the CSU Council on Ocean Affairs, Science & Technology (COAST), and Marin County DPW, all of which provided generous financial assistance that was critical to my ability to undertake this project and complete my graduate studies.

TABLE OF CONTENTS

List of Table.....	viii
List of Figures.....	x
Introduction.....	1
Research Approach.....	5
Climate Change and Flood Vulnerability in California.....	7
Novato Creek Watershed.....	8
Methods.....	11
Identification of Future Climate Scenarios.....	12
Global Climate Model Selection.....	12
GCM Precipitation Trend Analysis.....	15
Precipitation Intensity for Future Extreme Storms.....	16
Hydrologic Model.....	18
HEC-HMS Model Structure.....	18
Future Storm Modeling with HEC-HMS.....	19
Sea Level Rise Projections.....	21
Climate Change Scenarios for Compound Flood Modeling.....	22
Hydraulic Model.....	23
HEC-RAS Model Structure.....	23
Analysis of Hydraulic Model Output.....	25
Socio-Economic Impacts.....	27

Results and Discussion	31
Precipitation Trends	31
Flood Hazard.....	32
Peak Discharge.....	32
Flood Extent.....	33
Flood Depth	36
Socio-Economic Impacts and Vulnerability	38
Population and Social Vulnerability	38
Roads.....	39
Residential and Commercial Property	40
Critical Facilities.....	41
Conclusion	42
CMIP Acknowledgement.....	87
References.....	88

LIST OF TABLES

Table	Page
1. Climate change scenarios used to investigate changes in flood hazard and socio-economic impacts of compound flooding.....	45
2. “California GCMs” recommended by California Dept. of Water Resources for climate modeling for California	46
3. Projected two-day, 50-year storm magnitudes under RCP 4.5 for Novato Creek (LOCA cell# 6434) for each California GCM for three future time periods, with percentage change over historic period (1950-2005)	47
4. Projected two-day, 50-year storm magnitudes under RCP 8.5 for Novato Creek (LOCA cell# 6434) for each California GCM for three future time periods, with percentage change over historic period (1950-2005)	48
5. Projected two-day, 100-year storm magnitudes under RCP 4.5 for Novato Creek (LOCA cell# 6434) for each California GCM for three future time periods, with percentage change over historic period (1950-2005).....	49
6. Projected two-day, 100-year storm magnitudes under RCP 8.5 for Novato Creek (LOCA cell# 6434) for each California GCM for three future time periods, with percentage change over historic period (1950-2005).....	50
7. Probabilistic sea level rise projections under RCP 8.5 emissions scenario	51
8. Socio-economic impact indicators and GIS data sources	52
9. Projected changes in two-day storm magnitude based on RCP 8.5 10-GCM ensemble mean change factors, compared to historic storm magnitudes and frequencies.....	53
10. Peak discharge in Novato Creek at selected upstream and downstream cross-sections under different climate change scenarios	54

11. Modeled changes in flood extent due to mid-century RCP 8.5 precipitation change projections for 10 California GCMs with no change in SLR.....	55
12. Modeled change in flood extent due to mid-century RCP 8.5 precipitation change projections for subset of four California GCMs plus SLR projections.....	56
13. Total population and socially vulnerable populations exposed to flooding from two-day, 50-year storm under different compound flood scenarios.....	57
14. Critical facilities exposed to flooding from two-day, 50-year storm under different climate change and compound flood scenarios.....	58

LIST OF FIGURES

Figures	Page
1. Map of San Francisco Bay showing location of Novato Creek watershed in Marin County north of the City of San Francisco	59
2. Elevation map of Novato Creek watershed	60
3. Types of land use within Novato Creek watershed	61
4. Outline of Novato Creek watershed and stream channels, showing boundaries of 1/16 degree LOCA downscaling grid and cell numbers, sub-basins used in HEC-HMS hydrologic model, HEC-RAS 2D flow areas for the Upper Creek and Lower Creek/Baylands, and locations of weather stations, stream gages, and channel discharge measurement locations	62
5. Comparison of gridded LOCA observed data vs. total annual precipitation from weather station point observations for corresponding periods of record at locations of Novato Library county rain gage and CIMIS station 063	63
6. Distribution of change factors for two-day 50-year storm from 10 California GCMs for three LOCA downscaling grid cells	64
7. Map of inundation extents for 21 st Century sea level rise projections for Novato Creek watershed, relative to major highways and populated areas	65
8. Flood extent for all modeled combinations of precipitation change and SLR for two-day, 50-year storm under RCP 8.5	66
9. Time series of annual total rainfall 1950-2100 under RCP 4.5 and RCP 8.5	67
10. Time series of number of wet days per year, 1950-2100	68
11. Change in annual maximum daily precipitation under RCP 4.5 and RCP 8.5	69
12. Changing distribution of total seasonal precipitation by time period for RCP 8.5 10-GCM ensemble mean	70
13. Changing distribution across 10 GCMs of projected two-day storm magnitude for 50-year and 100-year storms under RCP 8.5	71

14. Modeled change in channel flow as a function of change in precipitation magnitude for mid-century (2040-69) 50-year, 48-hour storm for each GCM, RCP 8.5	72
15. Novato Creek historic peak discharge and flood stage	73
16. Change in flood extent as a function of change in precipitation magnitude for two-day, 50-year storm under RCP 8.5 with no SLR	74
17. Flooded area in the Novato Creek upper watershed by duration of flooding, comparing the historic 50-year storm with mid-century and late-century compound flood scenarios	75
18. Flood duration in Novato Creek upper watershed under Scenario C	76
19. Modeled compound flood extent in the upper watershed only, for different SLR as a function of changes in 50-year storm magnitude under RCP 8.5	77
20. Comparison of Scenario A compound flood extent to area inundated by 0.6 m (1.9 ft) SLR and flood extent of historic 50-year storm	78
21. Flood extent by climate change scenario for two-day, 50-year storm	79
22. Distribution of flood depth by changing storm magnitude with no change in sea level	80
23. Comparison of effects of historic 50-year storm, SLR and compound climate change scenarios on distribution of flood depth	81
24. Distribution of flood depth by area flooded in the Novato Creek upper watershed, comparing the historic 50-year storm with mid-century and late-century compound flood scenarios	82
25. Distribution of low-income population by census block groups, relative to Scenario A (mid-century) and Scenario C (late-century) compound flood extent	83
26. Length of flooded roadway showing changes under different scenarios for SLR and a 50-year, two-day storm under RCP 8.5	84

27. Number of inundated buildings by type of use, showing changes under different scenarios for SLR and a 50-year, two-day storm under RCP 8.585

28. Map of Upper Novato Creek watershed showing location of buildings, critical facilities and major roads relative to flooding under historic 50-year storm and compound flood Scenarios A and C86

INTRODUCTION

This study investigates the effects of climate change on compound fluvial and coastal flooding, using coupled hydrologic and hydraulic models to examine the changing physical characteristics and socio-economic impacts of flooding in a small basin typical of many flood-prone areas on the United States (U.S.) west coast. Recent research on climate change indicates that by the end of the 21st century global sea level will rise at least 0.5 m (1.6 ft), and could reach as much as 3 m (10 ft) under the most extreme projections of rapid ice-sheet loss in Antarctica (Kopp et al., 2014; Sweet et al., 2017). Simultaneously, heavy precipitation events are projected to increase in frequency or intensity in most parts of the world (Chen et al., 2018; IPCC, 2013), contributing to significant changes in global flood risk, although the scale and direction of change in flooding will vary substantially by region (Arnell and Gosling, 2016; Kundzewicz et al., 2014). Many efforts are underway to map and assess U.S. vulnerability to coastal flooding from sea level rise (SLR), both nationally (Climate Central, 2019; Dahl et al., 2018, 2017; NOAA, 2018) and for California (Ballard et al., 2016; BCDC, 2017). In California, where 70% of the state's 39.5 million residents live in coastal counties, the San Francisco Bay Area and selected coastal communities in the greater Los Angeles region are most at risk (Barnard et al., 2019; Dahl et al., 2018, 2017; Strauss et al., 2014, 2012). Multiple studies have also investigated the effects of climate change on precipitation and fluvial flooding in California, finding large increases in storm magnitudes and flood flows even as precipitation becomes less frequent and drought

periods become longer and hotter (Das et al., 2013; Dettinger, 2011; Dettinger et al., 2016; Maurer, 2007; Maurer et al., 2018; Pierce et al., 2018, 2013; Russo et al., 2013; Swain et al., 2018). Less is understood about the physical processes of compound fluvial and coastal flood events. As climate change accelerates, it is becoming more urgent to understand these compound processes, particularly to anticipate the effects of changing precipitation and sea level in communities where rivers and streams meet the coast.

Compound flood events occur when multiple drivers of flooding, whether individually extreme or not, coincide to create extreme impacts (Hao et al., 2018; Leonard et al., 2014). Compound events can also be driven by fires, droughts, high winds and other climate extremes, as well as by social and economic conditions (Zscheischler et al., 2018). There is some evidence that compound events are occurring more frequently globally (Wahl et al., 2015), and there is growing consensus on the need to expand research on the probabilities and impacts of compound events (Chen et al., 2018; Hao et al., 2018; Zscheischler et al., 2018). Within this emerging body of research, most studies have focused on identifying appropriate multivariate statistical methods to take into account the dependencies between extreme events when quantifying compound probabilities (Couasnon et al., 2018; Moftakhari et al., 2017; Petroliagkis et al., 2016; Ward et al., 2018; Zheng et al., 2014). Only a small number of studies have modeled the physical processes of compound events (Chen and Liu, 2014; Ikeuchi et al., 2017; J. Lian et al., 2013; Kumbier et al., 2018; Olbert et al., 2017; van den Hurk et al., 2015), and

even fewer have incorporated climate change effects into the models. Orton et al. (2018) and Pasquier et al. (2018) modeled compound coastal and fluvial flooding incorporating SLR only, while Kew et al. (2013) and Klerk et al. (2015) modeled compound effects of changes in storm surge and extreme precipitation. Webster (2014) modeled compound fluvial flooding, SLR and storm surge, and did an additional statistical analysis of the effect of climate-driven changes in fluvial flows. For the San Francisco Bay, Erikson et al. (2018) included fluvial discharge projections for the Sacramento/San Joaquin Delta and eight large local rivers, along with projected SLR, storm surge and tidal variability, in their model of climate change effects on coastal flooding, but local river discharges input to the model were derived statistically based on modeled Delta flows. Modeling studies that incorporate changes in multiple flood drivers can provide insights about the physical characteristics and processes of compound events under changing climate conditions that are different from and complementary to statistical probability analyses.

Modeling compound flood events also provides information on the physical dimensions of flood exposure that allow for detailed assessment of community vulnerability. Flooding is the most common type of natural hazard in the U.S. and worldwide with enormous social and economic consequences (UNISDR, 2015). Data compiled by the National Weather Service shows an average of 82 lives lost and nearly \$8 billion in damage annually in the U.S. over the 30-year period up to 2014, without including the catastrophic 2017 hurricane season (Blunden et al., 2018; NWS, 2015). Globally, 43% of

weather-related natural disasters that occurred between 1995-2015 were floods, impacting 2.3 billion people and causing 157,000 deaths and \$662 billion in damages (UNISDR, 2015). Climate change and continuing urban development in floodplains will increase these consequences significantly absent efforts to reduce risk and increase resilience to changing flood hazard. Vulnerability assessment is a useful starting point for such efforts. Vulnerability is the potential for damage or injury due to both the exposure of communities and people to flood hazard and their sensitivity and adaptability to such exposure (Adger, 2006). Vulnerability is often categorized into biophysical, economic and social components, and there is substantial research literature focused on identifying measurable indicators and crafting indices and scorecards to compare vulnerability across time and place (Cutter, 2016; Nguyen et al., 2016). The most commonly used indicators measure population, property, roads, and other critical infrastructure, such as power facilities and emergency services (Jones et al., 2016; Strauss et al., 2014). There is also a growing focus on social vulnerability, which analyzes population characteristics, such as income, age, race/ethnicity, as well as concepts such as community social capital, to understand differential abilities to prepare for, respond to, and recover from flooding or other hazards (Cutter et al., 2003; Cutter and Emrich, 2017; Flanagan et al., 2011; Fothergill and Peek, 2004; Thomas et al., 2019; Wein et al., 2016). Vulnerability assessment provides essential information for community planning to mitigate risk and increase resilience in advance, and to prepared for successful emergency response in the event of a disaster.

RESEARCH APPROACH

In this study, I use coupled hydrologic and hydraulic models to evaluate the compound effects of future extreme precipitation and SLR on flood magnitude and frequency for Novato Creek, a coastal watershed located in Marin County, California along the northeastern edge of the San Francisco (SF) Bay (Figure 1). My primary research question is: what are the changes in flood extent and socio-economic vulnerability due to climate change effects on compound fluvial and coastal flooding along Novato Creek? I also ask how the effects of compound flooding differ from those of SLR or changing precipitation and streamflow alone.

Similar to many bays and deltaic systems globally, SF Bay and its surrounding watersheds are highly vulnerable to climate change (Ackerly et al., 2018; Strauss et al., 2014). Novato Creek is densely populated and highly engineered, like most other watersheds in Marin County and elsewhere in SF Bay, leaving little space for any increase in flood waters. Even without climate change, portions of the Novato Creek flood control structures do not fully contain the storms for which they were designed. Therefore, the findings from this study will provide important guidance for local and regional flood managers, planners and policymakers as they plan for the next generation of flood protection measures and work to increase resilience. In addition, the methods in this study may be useful in demonstrating techniques for incorporating more comprehensive local climate change effects into flood risk mapping. Currently, official

Federal Emergency Management Agency (FEMA) flood maps are beginning to include supplemental non-regulatory information showing how 1 to 3 feet of SLR will change flood extent for 100-year storms. But FEMA maps do not incorporate climate change effects on streamflow, nor does FEMA provide regulatory guidance on scientific methods for comprehensive assessment of climate change effects in flood risk studies. This study may also offer insights on broader questions about compound flood hazard sensitivity and the relative control of fluvial and coastal processes in coastal watersheds with similar terrain.

To model climate change effects on compound flooding, I analyzed downscaled precipitation data from multiple global climate models (GCMs) to create projections of future extreme storm magnitudes for the Novato Creek watershed. I also obtained the latest SLR projections for SF Bay through the year 2100. I used these projections to adjust the boundary conditions of hydrologic and hydraulic models previously developed by the Marin County Department of Public Works (MCDPW), producing projections of flood hazard for four different future climate scenarios (Table 1). I then evaluated the socio-economic impacts of these flood scenarios by compiling measures of affected population, property and infrastructure, including potential differential impacts on socially vulnerable residents.

CLIMATE CHANGE AND FLOOD VULNERABILITY IN CALIFORNIA

In California, climate change is projected to significantly increase extreme precipitation, flood hazard and vulnerability (Dahl et al., 2017; Das et al., 2013; Dettinger, 2011; Maurer et al., 2018; Pierce et al., 2018; Swain et al., 2018; Warner et al., 2014). Studies of the effects of climate change on precipitation patterns in California have consistently projected significant growth in interannual variability, pronounced seasonal shifts (e.g., Pierce et al. (2018) project up to 20% increases in winter precipitation together with 20% decreases in spring and fall), and increasing frequency and magnitude of extreme storms, alongside relatively little increase in total annual precipitation. Notably, atmospheric rivers, the driver of most of the largest floods in California are projected to increase in frequency and magnitude (Dettinger, 2011; Warner et al., 2014). Swain (2018) projects a 100 – 200% increase in extreme wet seasons and a 300 – 400% increase in frequency of extreme flood events in California by the end of the century. Das et al. (2013) projected 30 – 100% increases in 50-year flood magnitudes on the western slopes of the Sierra Nevada mountains in California, and Maurer et al. (2018) projected 31% – 43% increases in peak streamflow on average across the western United States (U.S.) by end of century. Climate change will also increase extreme sea levels as larger storm surges combine with SLR (Cayan et al., 2008). Research indicates that current 100-year storm surges along the coast of California could occur as often as every 1 to 20 years by mid-century (Tebaldi et al., 2012).

Recent estimates of vulnerability to SLR in California found that 109,000 residences housing 273,000 people will experience chronic inundation¹ by 2100 (Dahl et al., 2018). When an extreme storm combines with SLR, over 600,000 people and \$150 billion of property could be impacted (Barnard et al., 2019). In the San Francisco Bay Area, San Mateo and Marin counties have the greatest vulnerability in terms of people and economic assets in low-lying areas (Climate Central, 2019; Dahl et al., 2018). Marin, San Mateo, Alameda and Contra Costa counties have all completed in-depth SLR vulnerability studies, but none have incorporated modeling of climate change effects on local streamflow and consequent compound flooding.

NOVATO CREEK WATERSHED

Located across the Golden Gate Bridge just north of San Francisco, CA, Marin County is bounded on the west by the Pacific Ocean and on the east by SF Bay (Figure 1). Novato Creek is the largest watershed in eastern Marin County with six major tributaries covering 125 km² (48 mi²). Beginning at over 425 m (1,400 ft) elevation in the ridges of the Northern California Coast Range, the main channel of Novato Creek flows east, through residential and commercial areas of the City of Novato, and empties into San Pablo Bay, a tidal estuary that forms the northern part of SF Bay (Figure 2). The watershed is 50% urbanized and more than 90% of development is residential. The

¹ Chronic inundation is defined as flooding that occurs 26 times or more per year (Dahl et al., 2018).

population of approximately 62,000 people is 75% white, 7% Asian, 2% Black and 16% other race/ethnicity. Nineteen percent (19%) identify as Hispanic or Latino (U.S. Census Bureau, 2019).

The Novato Creek watershed is characteristic of many bay and coastal areas in California with widely varying topography and land use (Figure 3). The upper watershed consists of steep, unpopulated hills surrounding Stafford Lake, a reservoir created by construction of a small dam that provides local water supply and flood control. Below the dam, Upper Novato Creek is narrow and deeply incised as it passes through residential neighborhoods and downtown Novato. Below downtown, the topography flattens out and Lower Novato Creek is highly engineered as it widens and passes between levees surrounded by detention basins and tidal marshes. Two major highways – U.S. Route 101 (US 101) and CA State Route 37 (CA-37) – as well as large power lines run through this low-lying area known as the Baylands. While the Baylands is less populated than upstream, it contains several commercial developments along with Bel Marin Keys, a large residential waterfront community.

The regional Mediterranean climate is characterized by mild rainy winters and hot dry summers, with extremes that already cause floods and wildfires on a regular basis. High tide or “nuisance” flooding is also becoming more common (Hino et al., 2019; Moftakhari et al., 2015). Flooding, when it occurs, usually happens in the winter. In

recent decades, major floods have inundated parts of downtown Novato in 1982, 1986, 1998 and 2006. Localized flooding has occurred in many other years, including most recently in winter 2017 and 2019 when heavy rains caused levee breaks, flooding portions of CA-37 for several days.

In 2017, Marin County completed an assessment of bay shoreline vulnerability to SLR (BVB Consulting, 2017). The assessment used six difference scenarios of combined SLR and storm surge to develop detailed inventories of the housing, transportation, utility infrastructure and other assets that could be inundated by rising tides. In most scenarios, large proportions of the Baylands are entirely inundated by SLR, although most of these lands are tidal marshes, stormwater detention basins, agricultural or open space. However, the study identified near-term vulnerability for the major highways, regional rail tracks and a wastewater treatment plant within the Novato Creek watershed. The vulnerability assessment did not model any change in precipitation patterns and therefore did not include climate change impacts on flooding upstream where most of the residential development is located, thus likely underestimating total climate change vulnerability and damage potential.

METHODS

In this study, I modeled future channel flows and resulting flood hazard for the Novato Creek watershed for a wide range of changes in precipitation and SLR. All scenarios were based on changes to the 48-hour, 50-year (2% annual chance of occurrence) design storm used by MCDPW for Novato Creek flood control planning. My methods were comprised of the following steps:

- 1) select GCM data to determine future precipitation conditions for the study area;
- 2) determine future extreme precipitation projections from GCM data;
- 3) use GCM projections to scale 50-year design storm to serve as hydrologic model forcings;
- 4) select SLR projections appropriate for the study location and time period;
- 5) establish combined precipitation and SLR climate change scenarios for compound flood modeling;
- 6) setup hydraulic model boundary conditions using hydrologic model outputs and selected SLR projections to match climate change scenarios;
- 7) evaluate coupled hydrologic and hydraulic model results to assess changes in channel discharge, flood extent, and depth; and
- 8) examine socio-economic impacts, including differential impacts on socially vulnerable populations.

The methods for these steps are described below.

Identification of Future Climate Scenarios

Global Climate Model Selection

Global Climate Models (GCMs) are three-dimensional (3D) mathematical simulations of the physical and chemical processes occurring within and between the earth's atmosphere, ocean and land. To facilitate public access and comparative research, The World Climate Research Programme coordinated the Coupled Model Intercomparison Project Phase 5 (CMIP5) experiments (Taylor et al., 2011), which included the development of an online archive of GCM model runs conducted using a standard set of climate forcings. Models in the CMIP5 use four standard forcing scenarios known as Representative Concentration Pathways (RCPs). RCPs are future levels of total radiative forcing due to changing concentrations of atmospheric aerosols and greenhouse gases. The four scenarios are RCP 2.6, RCP 4.5, RCP 6 and RCP 8.5 (Moss et al., 2008). RCP 4.5 is a stabilization scenario based on emissions beginning to level off and then decline after mid-century, while RCP 8.5 assumes that emissions continue increasing at current rates through the end of the 21st century. For this project, I determined precipitation projections for Novato Creek for both the RCP 4.5 and RCP 8.5 scenarios. But I used only the RCP 8.5 data for flood modeling given that global emissions are currently consistent with higher emissions scenarios and not on track to decline (Brown and Caldeira, 2017; USGCRP, 2017). In addition, since RCP 4.5 levels off after mid-century,

RCP 8.5 projections for mid-century can be seen as an approximation of RCP 4.5 late-century conditions (Franco et al., 2018).

Climate change studies often use an ensemble of multiple GCMs, preferably at least ten (Maurer et al., 2014; Mote et al., 2011; Pierce et al., 2009), to capture the range of variability and uncertainty in model projections. For GCM output to be applied to practical water resource or other environmental management issues at the regional or local level, the data must be downscaled to finer spatial resolution and “bias-corrected”. Bias correction is a statistical technique to adjust the large-scale model output to reflect smaller scale climate characteristics, often by assimilating more localized information about topographic variability and historical climate observations. Using downscaled GCM data is especially important for climate change studies in California where coastal and orographic influences can cause large changes in climate across small distances.

The California Department of Water Resources (DWR) recommends that climate change studies in California use a set of 10 GCMs (Table 2) (DWR, 2015) from the CMIP5 archive that were downscaled and bias-corrected using the Localized Constructed Analogues (LOCA) statistical method (Pierce et al., 2015, 2014). DWR determined that the LOCA data from these 10 “California GCMs” best simulate climate dynamics across California based on a set of global, regional, and state level criteria. LOCA data products

are the highest resolution downscaled GCM products currently available, with daily precipitation projections provided in a 1/16 degree (approximately 6 km or 3.7 miles) grid for the conterminous U.S. The LOCA data include historical model runs for the years 1950 to 2005 and model projections for the years 2006 to 2100 for each GCM for RCP 4.5 and RCP 8.5. An additional observed data product for each LOCA grid cell provides interpolated values from station observations for the historic period from 1950 to 2005 (Livneh et al., 2015). This gridded observed data was used by the LOCA developers to calibrate the GCM downscaling for the historic period before producing the projected datasets. In August 2018, the California GCMs were endorsed in the California Fourth Climate Change Assessment (Pierce et al., 2018), which further recommended a subset of four GCMs to be used for projects that do not have the resources to analyze all 10 GCMs (Table 2). Based on these DWR recommendations, I selected the 10 California GCMs to model future hydrology for this study.

To obtain the raw GCM data, I downloaded the LOCA daily historic observed data and precipitation data for the RCP 4.5 and RCP 8.5 emissions scenarios for the 10 California GCMs from the CMIP5 online archive (“Downscaled CMIP3 and CMIP5 Climate and Hydrology Projections,” 2016) for three of the LOCA grid cells spanning the east (cell# 6435), center (cell# 6434) and west (cell# 6345) of the watershed (Figure 4). I then tested the LOCA historic observed data against reported data from local weather stations to check if the modeled data were sufficiently accurate for the local area or needed further

bias-correction. There are only two weather stations within the Novato Creek watershed that have precipitation records for at least 10 years prior to 2005 as needed to permit valid comparison. As shown in Figure 4, the Novato Library Rain (gage #38027) operated by Marin County is located within LOCA cell# 6434 near the center of the watershed. The second gage, Novato CIMIS 063, operated by the California Irrigation Management Information System (CIMIS), is located downstream just outside the northern boundary of the watershed within the eastern LOCA grid cell# 6435. As shown in Figure 5, total annual precipitation from the LOCA observed data follow a similar pattern as the gage observations. A Wilcoxon signed-rank test (alpha level = 0.05) did not find a significant difference between the LOCA observed and gage data distributions for either the Novato Library ($p = 0.05$) or CIMIS063 ($p = 0.85$) locations, indicating that no further bias-correction of the downscaled GCM data was necessary.

GCM Precipitation Trend Analysis

To understand the trends projected for rainfall in the Novato Creek watershed, I analyzed changes in the 10-GCM ensemble means for total annual and seasonal rainfall, annual peak daily rainfall, and number of wet days per year. This analysis focused on data from the single LOCA grid cell# 6434 at the center of the watershed (Figure 4), which encompasses the Novato Library rain gage and the adjacent county and U.S. Geological Survey (USGS) stream gages. For most analyses, I determined annual values based on water year (October 1 to September 30) rather than calendar year. I examined total annual

precipitation and daily peak rainfall magnitude for significant linear trends across the entire time period 1950-2099. I also divided the modeled GCM data into approximately 30-year time-periods—early-century/current period 2006-2039, mid-century 2040-2069, and late-century 2070-2099—for comparison against the base period of the historic observed data 1950-2005. I used the entire period of the historic observed data for the base period, rather than a 30-year period (e.g., 1976-2005), because the longer period aligns with the source data for the modeled historic design storms.

I also analyzed seasonal patterns in the data using three-month periods beginning in September, December, March, and June. These seasonal periods are designed particularly to capture the peak of the California wet season from December to February. To obtain ensemble mean values for each 30-year period, I calculated the precipitation values for each GCM for each year, then calculated an ensemble mean for each year, then applied ANOVA and Student's t-tests to compare the means and variances of the distributions for each time period.

Precipitation Intensity for Future Extreme Storms

The final step in establishing future precipitation projections was to determine rainfall intensities for extreme storms, in this case for the 100-year and 50-year return periods (1% and 2% annual exceedance probabilities) used for flood model design storms. The design storms for the MCDPW hydrologic model of Novato Creek are based on a two-

day event that occurred around New Year's Day 2006. Using an annual maximum series (AMS) method, similar to the approach used in NOAA Atlas 14 (Perica et al., 2014), I began by constructing time series of annual peak two-day precipitation for every GCM for RCP 4.5 and RCP 8.5. I then fit these annual maxima to the Gumbel (Type I) extreme value distribution to obtain intensity-duration-frequency (IDF) curves for each GCM. Using the transformation of the Gumbel distribution function as shown in Equation 1, I calculated the projected two-day storm magnitude for the 100 and 50-year return periods from the mean and standard deviation of the AMS for each 30-year period. I then used this data to create change factors for each GCM and each future period (Tables 3 – 6) by calculating the percentage change in the magnitude of each future storm, relative to the historic base period storm of the same duration and frequency as shown in Equation 2. These change factors were then used to adjust the design storm hyetographs as explained below.

Equation 1: $X_T = \bar{X} + K_T S$

Where: X_T is the value in the distribution for the given return period

\bar{X} is the mean

S is the standard deviation

T is the return period

$$K_T = -\frac{\sqrt{6}}{\pi} \left[0.5772 + \ln \left(\ln \left(\frac{T}{T-1} \right) \right) \right]$$

$$\text{Equation 2: } \textit{Change Factor}_{\textit{future period}} = \frac{X_{T \textit{future period}} - X_{T 1950-2005}}{X_{T 1950-2005}}$$

Hydrologic Model

HEC-HMS Model Structure

To model the routing of storm runoff in the Novato Creek watershed, I used a hydrologic model provided by MCDPW (Leventhal, 2013; Mueller, 2013). The Novato Creek model was built using the USACE Hydrologic Engineering Center's Hydrologic Modeling System (HEC-HMS) software (USACOE, 2016a). In the model, the watershed is divided into 34 sub-basins (Figure 4) and the user provides storm hyetographs for each sub-basin. The model output are flow hydrographs for each sub-basin, which I used as inflows to the channel hydraulic model.

When initially constructed, the Novato Creek hydrologic model was calibrated for a two-day storm that occurred around New Year's Day 2006. Hyetographs for each sub-basin were derived by interpolating sub-hourly precipitation data for the 2006 storm from several nearby rain gages (Mueller, 2013). These 2006 sub-basin storm hyetographs were subsequently translated into unit hyetographs, allowing the model to be run for storms of other magnitudes by entering the total two-day precipitation for each sub-basin. To setup the model for 100-year and 50-year design storms, two-day rainfall magnitudes with 1% and 2% annual chance of occurrence were obtained for the centroid point of each sub-

basin from NOAA Atlas 14 point precipitation frequency estimates (Mueller, 2013). The HEC-HMS infiltration loss parameters and sub-basin hyetographs were further adjusted to calibrate the output to 100-year and 50-year discharges for Novato Creek based on flood frequency curves derived from Novato Creek USGS stream gage data. The design storm models also include settings for the antecedent conditions, including assumptions that Stafford Lake is full at the start of the model run (so dam overflow begins immediately) and that the ground is relatively saturated (low loss ratios). Complete details of the HEC-HMS model structure and calibration can be found in Appendix D of Kamman Hydrology (2014).

Future Storm Modeling with HEC-HMS

Given the extent of the previous calibration around these specific design storms, I chose to use a quantile perturbation approach to represent projected future hydrology, rather than enter the GCM projection data directly into the HEC-HMS model. This method of perturbing IDF relationships has been shown to produce credible values for hydrologic impacts analysis (Ntegeka et al., 2014; Willems and Vrac, 2011). To establish projected hyetographs for 50-year storms under the RCP 8.5 climate scenario for each GCM and future time period, I multiplied the 50-year design storm sub-basin totals by the 50-year storm change factors from Table 4. I applied the same change factor, derived from LOCA cell# 6434 located at the center of the watershed, to all sub-basins. To be more spatially precise, the change factor applied to each sub-basin hyetograph could have been derived

from the LOCA grid cell that best coincides geographically with each sub-basin or from a weighted average of all the grid cells overlapping each sub-basin. However, my simplification is unlikely to have a significant impact on the results because the differences in change factors across grid cells are much smaller than the differences in values across all the GCMs within each cell. Further, as shown in Figure 6, I found no significant differences (ANOVA, p -value = 0.998, alpha-level = 0.05) among the ensemble mean change factors from LOCA cells located further east and west in the watershed, where different topography and coastal proximity could be expected to affect rainfall patterns.

All other basin characteristics were unaltered for the future storm models. Although there could well be changes in the watershed landscape in the coming decades, such as increases in impervious surface from increased urbanization, or changes in vegetation cover as the climate changes, projections for these types of changes were not available and therefore I did not alter impervious surface or roughness settings in HEC-HMS. Similarly, no changes were made to antecedent lake reservoir or soil moisture conditions. Although future increases in temperatures could create drier antecedent conditions, historically the wettest winter periods have been characterized by back-to-back storm events such that flooding events would likely be generated by storms that begin with saturated conditions. Given the goal of this study to model the impacts, not probabilities,

of extreme future events, I maintained the relatively wet antecedent conditions in the original model design.

Sea Level Rise Projections

The latest research looking across a wide variety of GCM data indicates that global sea level will rise at least 0.5 m (1.6 ft) by 2100 (Kopp et al., 2017, 2014; Sweet et al., 2017). In the SF Bay, SLR is projected to rise from 0.2 to 0.8 m (0.7 to 2.7 ft) by 2050 and 0.5 to 3.1 m (1.6 to 10.2 ft) by 2100 (Griggs et al., 2017; NOAA, 2018; Pierce et al., 2018). These values correspond to a range of probability levels as shown in Table 7. For this study, I focused on the Intermediate/Likely Range (66% probability) SLR projections for the later ends of the 30-year time periods used in developing the GCM precipitation projections: 0.6 m (1.9 ft) by 2070 and 1 m (3.4 ft) by 2100. These projections also correspond to high-risk/low-probability (0.5%) projections for the earlier end of each time period, thus covering the range of risk aversion recommended in state guidance from the California Ocean Protection Council (OPC, 2018). I also investigated one extreme SLR scenario of 1.6 m (5.2 ft) by 2070.

In addition to SLR, storm surge will be an important component of future flood hazard. Storm surge is a major contributor to coastal flooding, especially when it is coincident with extreme precipitation events. In the SF Bay, storm surges currently can exceed 1 m

(3 ft) (AECOM, 2016; BCDC, 2017), and are projected to increase with climate change (Ballard et al., 2016; Barnard et al., 2019; Tebaldi et al., 2012). The Adapting to Rising Tides (ART) Bay Shoreline Flood Explorer (BCDC, 2017) uses a 50-year storm surge height of 1 m (3 ft) in its SLR projections. Marin County's recent Bay shoreline SLR vulnerability assessment included 100-year storm surge scenarios of approximately 1.4 m (4.7 ft) by 2050 and 2.4 m (8 ft) by 2100 (BVB Consulting, 2017). As has been done in other studies of SLR impacts (BCDC, 2017), I did not separate SLR and storm surge projections in setting the tidal boundary condition for hydraulic modeling in this study. However, the modeled sea levels can also be considered total water levels and allocated as various combinations of SLR and storm surge. For example, SLR of 1 m (3.4 ft) or 1.6 m (5.2 ft) can also be static approximations of 0.6 m (1.9 ft) SLR plus storm surge of 0.4 m (1.5 ft) or 1 m (3.3 ft) respectively, which are within the range of projections for future 50-year return period storm surges.

Climate Change Scenarios for Compound Flood Modeling

Table 1 shows the four climate change scenarios used to drive compound flood modeling for this project. All scenarios use RCP 8.5 GCM projections. Scenarios A and B are intermediate and high mid-century scenarios, combining the mid-century 10-GCM ensemble, 30-year median precipitation projection with SLR projections of 0.6 m (1.9 ft)

and 1 m (3.4 ft). Scenario C is an intermediate late-century scenario, combining the late-century 10-GCM ensemble, 30-year median precipitation projection with 1 m (3.4 ft) SLR. Scenario D combines the late-century 10-GCM ensemble, 30-year median precipitation projection with 1.6 m (5.2 ft) SLR to represent an extreme mid-century scenario, as well as an intermediate-high late-century scenario.

Hydraulic Model

HEC-RAS Model Structure

The Novato Creek hydraulic model was developed in the USACE Hydrologic Engineering Center's Hydrologic River Analysis System (HEC-RAS) software (USACOE, 2016b) by Schaaf & Wheeler consultants for MCDPW (Schaaf & Wheeler, 2018a, 2018b, 2018c, 2017), based on previous work by Kamman Hydrology & Engineering and WRECO (KHE, 2014). The model consists of a one-dimensional (1D) channel flowing from Stafford Lake to San Pablo Bay and 15 two-dimensional (2D) flow areas (Figure 4). The large North and West flow areas cover the area of Upper Novato Creek, while the remaining 2D flow areas comprise the Lower Creek/Baylands area. Flow hydrographs from the HEC-HMS model serve as the upstream boundary condition inputs for the HEC-RAS model, while the downstream boundary is a stage hydrograph set to model tidal conditions at the channel outlet. To isolate the effects of SLR, I set the tidal boundary condition at a constant level rather than modeling daily tidal variability.

This is common practice in FEMA flood modeling studies, using the Mean Higher High Water (MHHW) level to capture effects of a rainfall event coincident with high tide (FEMA, 2009), although it can result in overestimates of flood depth in areas where outgoing tides would speed flood recession. The original HEC-RAS model provided by MCDPW had a MHHW boundary condition of 1.9 m (6.3 ft) based on historical conditions in SF Bay (Schaaf & Wheeler, 2018b). While I adjusted initial water level conditions in the model to match different SLR scenarios, I did not change the model geometry to account for changes in shorelines and intertidal processes that would occur at much higher sea levels, nor for potential future changes in levees or other flood control infrastructure. The model also does not incorporate how flood waters would flow around buildings or bridges as it was based on a bare earth digital elevation model (DEM) derived from high-resolution LiDAR.

To model the future compound flood scenarios, I ran the HEC-RAS model using the HEC-HMS hydrographs for each GCM as the upstream boundary conditions, and added SLR increases to the baseline MHHW of 1.9 m (6.3 ft) at the channel outlet. In addition, I set initial condition water levels within the channel and in the downstream 2D flow areas to match projected sea levels. To identify the specific areas where these downstream initial conditions needed to be adjusted, I used flood extents from online SLR viewers produced by Our Coast Our Future (OCOF)² and the Adapting to Rising Tides project³.

² <http://data.pointblue.org/apps/ocof/cms/index.php?page=flood-map>

³ <https://explorer.adaptingtorisingtides.org/home>

As shown in Figure 7, at 0.6 m (1.9 ft) of SLR, the detention ponds and marshes south of Lower Novato Creek will be permanently inundated. By 1 m (3.4 ft) SLR, most of the Baylands and CA-37 will be flooded at high tide. At 1.6 m (5.2 ft) SLR, Bay waters will cross into lower-lying commercial and residential developments west of US 101, flooding portions of the highway and reaching the confluence of Upper Novato Creek and Warner Creek. Under non-storm conditions, most of the rest of the upper watershed appears insensitive to SLR due the steepness of the topography. I did attempt to run the HEC-RAS model to investigate the possibility that more extreme SLR beyond 1.6 m (5.2 ft) could cause additional backwater effects upstream. However, by that stage, intertidal flows and other physical conditions in the watershed will no longer match the geometry in the HEC-RAS model geometry and the model generated errors making the results unreliable results.

Analysis of Hydraulic Model Output

To analyze the model output to determine the effects of the different climate scenarios on compound flood hazard, I used three indicators – peak discharge, maximum flood extent and flood depth. I extracted peak discharge from the HEC-RAS model at two cross-section locations –one upstream (HEC-RAS River Station (RS) 39926) corresponding to the location of the USGS stream gage, and one downstream (RS 32080) below the junction with Arroyo Avichi near where the Baylands area of the HEC-RAS model begins (Figure 4). To obtain flood extent, I extracted inundation boundary maps from

HEC-RAS representing all areas flooded to a depth of at least 152 mm (6 in) at any time during the simulation. Then I used GIS software to combine individual GCM results to obtain maps of the multimodel ensemble median flood depth and inundation extent for each SLR scenario. I also analyzed flood extent data separately for the upstream and downstream areas of the watershed, using the boundaries of the 2D flow areas in the HEC-RAS model to delineate the division between the upper and lower watershed flood areas as shown in Figure 4. For flood depth, I assessed changes by examining the distribution of flooded surface area by flood depth, with the expectation that higher rainfalls and SLR would shift the peak of the area distribution to higher depths.

My initial investigations showed that SLR had very little effect on upstream flood extent, at least up to 1 m (3.4 ft) SLR, and relatively limited upstream sensitivity at 1.6 m (5.2 ft) SLR. Additionally, downstream flood extent reached nearly the entire Baylands area by 1 m (3.4 ft) SLR before any change in precipitation was added. Therefore, it was not necessary to examine model results at higher SLR for every increment in GCM precipitation projections in order to discern the pattern of flood response. Given these findings, I reduced the model runs for scenarios with SLR, to only the subset of four California GCMs (Table 2). Because the four GCMs include the minimum and maximum changes in precipitation, they are sufficient to show the full range of flood response. Plotting these initial model results, as shown in Figure 8, I found that the relationship between precipitation increase and flood extent increase is nearly linear, with an

inflection point where the proportional response in flood extent changes at around 30% increase in precipitation. I also found that the linear relationship did not differ significantly based on the 4-GCM versus 10-GCM dataset, and that the 10-GCM (with no SLR) dataset produced a multimodel median flood extent that was consistent with the plotted linear pattern. Subsequently, I ran the model for a few additional test scenarios, which confirmed the linear relationship. Based on this finding, I was able to obtain additional median mid-century and late-century flood projections by initiating model runs with the 10-GCM ensemble median precipitation projections, rather than producing multimodel median results from all of the individual GCM data.

Socio-Economic Impacts

To analyze socio-economic impacts of flooding, I focused on identifying the number of people and critical infrastructure that could be exposed to flooding under Scenarios A – D compared to the historic 50-year storm and to SLR alone. The specific socio-economic indicators and source data are shown in Table 8. To measure impact, I used GIS software to extract the number of people or infrastructure located within the flood inundation boundary for each climate scenario. Limitations of the data include:

- *Population:* All population data are from the 2016 American Community Survey (ACS) which only provides data down to the area of census block groups. For this

study, I captured data for the Novato Census County Division (CCD), which is comprised of 31 census block groups that include the City of Novato, plus surrounding unincorporated communities. The area of the Novato CCD aligns very closely with the boundaries of the Novato Creek watershed, except that it includes one large block group that extends north along the eastern side of US 101 with much of that block group area falling well outside of the Novato Creek watershed. To estimate population in inundated areas, I converted the block group data to population density for each square foot, then multiplied by the number of square feet flooded. Because this method unrealistically assumes an even distribution of population throughout the entire block group, it may over- or underestimate the actual population living in the flood zone. Underestimates are particularly likely for the northernmost block group, since most of the population is concentrated in the southern portion of the block group that falls within the Novato Creek watershed, while the remainder of the block group area that is outside the watershed is mostly open space.

To identify people who may be vulnerable to flooding due to low financial resources, I used data on income relative to the federal poverty level (FPL). For 2016, the federal poverty level was \$11,880 for a single person and \$24,300 for a family of four. In Marin County, an affluent area where 2016 median per capita income was \$63,608, median household income was \$100,310, and the median

cost of housing was around \$2,000 per month, poverty level income is likely to be associated with other vulnerability factors such as living in substandard housing and flood-prone locations (Fothergill and Peek, 2004; Thomas et al., 2019). Although median incomes are lower in Novato, where the 2016 median per capita income was \$49,500 and median household income was \$86,508, they are still very high relative to the FPL and local housing costs. Thus, to capture flood vulnerability due to poverty, I examined data for populations with incomes below both 100% and 200% of the FPL.

- *Roads*: Road data counts mileage in each direction separately for multi-lane highways and includes frontage roads, fire roads, service roads, driveways, trails, walkways, and railroad lines and docks that may have restricted access. In addition, major roads counts each direction separately for US 101. Hence, total roadway miles may overestimate the extent of restriction to local mobility. Bridges were not taken into account in the HEC-RAS model, so elevated bridges may not be underwater even when they appear to be in the flood extent maps. However, in most cases the bridges will be effectively out of service because surrounding access roads and on-ramps will be under water.
- *Facilities*: Building footprint data from Marin County is based on outlines derived from high-resolution aerial photography. It is more precise than analysis using

parcel data, since parcels will be indicated as flooded whether the flooded portion of the parcel contains a building or is open space (e.g., front yard, parking lot). However, the analysis does not consider whether buildings are raised above ground level and thereby above the flood depth since such data was not available. Critical facilities were identified by Marin County and include emergency services (police, fire, and City Hall), hospitals and medical centers (including clinics and mental health facilities), schools and community centers (including child care centers), and utilities (wastewater treatment plants and power substations). In some cases, critical facilities are not properly identified as exposed to flooding because the data are point locations that don't correspond to entire building footprints.

RESULTS AND DISCUSSION

Precipitation Trends

My analysis of the downscaled GCM data indicates that under the RCP 8.5 emissions scenario, precipitation in the Novato Creek watershed will become more variable and storms will grow more intense through the middle and end of the 21st Century. Mean annual precipitation is projected to increase 17% by late-century (Figure 9). At the same time, the number of wet days per year will decrease slightly (Figure 10), while peak daily precipitation will increase (Figure 11), suggesting there will be fewer, but larger storms. Further, these storms may be concentrated in a shorter winter rainy season each year, as mean total winter season precipitation is projected to increase 34% by late-century, while mean total fall season precipitation will decline 16% (Figure 12). These findings of shorter, wetter winters and growing storm magnitudes are consistent with broader studies of expected climate change in California as described earlier. In addition, my analysis indicates that Marin County will experience greater increases in total precipitation than the state as a whole, which is also consistent with historical patterns of higher rainfall in northern California relative to other parts of the state as well as with other climate change studies.

Moving to extreme storm events that generate flooding in Novato Creek, Figure 13 shows that there will be significant increases in the magnitude of 50 and 100-year storms by mid and late-century under RCP 8.5. The 10-GCM ensemble mean magnitude for a two-day, 50-year storm will increase $16.2\% \pm 5.9\%$ by mid-century and $30.5\% \pm 7.8\%$ by late-century under RCP 8.5. According to historic period data from NOAA Atlas 14 intensity-duration-frequency (IDF) curves⁴ for the location of the Novato Library rain gage, the intensity of a two-day storm with a 50-year return period is 211 mm (8.3 in) and a 100-year storm is 236 mm (9.3 in). As shown in Table 9, which applies the 10-GCM ensemble mean change factors for RCP 8.5 to the Atlas 14 storm magnitudes, by mid-century a 50-year storm is likely to meet or exceed the magnitude of the current 100-year storm and could approach the magnitude of the current 200-year storm. By late-century, 50-year storms could reach the magnitude of current 500-year storms.

Flood Hazard

Peak Discharge

Peak discharge in Novato Creek responds to precipitation changes differently upstream and downstream. Upstream, peak discharge increases as precipitation increases, but levels out once storm magnitudes increase more than about 10% over the design storm (Figure 14). This leveling of peak discharge can be attributed to the fact that the

⁴ https://hdsc.nws.noaa.gov/hdsc/pfds/pfds_map_cont.html

estimated flood stage is 2,570 cfs (Figure 15) and most flow beyond that leaves the channel. However, much of this overland flow eventually reenters the wider downstream channel, leading to steadily increasing discharge in the lower creek as precipitation increases. As shown in Table 10, SLR has no effect on discharge upstream. In order to test the boundary of SLR influence, downstream discharge data was extracted at a point just below the confluence of Arroyo Avichi and the main stem where the channel widens and flow transitions from the upper to lower creek. At this point, there is also very little change in discharge regardless of SLR. Model results indicate that at 1m (3.4 ft) SLR and higher, storm discharge will begin to slow in the lower reaches of the channel below CA-37, but errors generated within the model by such high initial water levels make this finding unreliable. Nevertheless, such slowing would make sense given that flows in the lower channel will effectively be encompassed by the Bay at that point in time.

Flood Extent

Flood extent in the Novato Creek watershed increases in nearly linear proportion to increases in storm magnitude. As shown in Table 11 and Figure 16, which examine change in flood extent as a function of change in the 50-year storm magnitude without any compound SLR effects, flooding in the upper watershed increases at approximately twice the rate of increase as in the Baylands and proceeds upward continuously. In contrast, flooding in the Baylands begins to level out once precipitation increases exceed about 30%. This inflection point in the growth of downstream flood extent probably

reflects the presence of flood control structures and the water levels at which most levees will be overtopped. Given that the Baylands accounts for 85% to 90% of the total flooded area across all model runs, total watershed flood extent follows a pattern very similar to the Baylands (Figure 16). With flood extent defined as all area where flood depth reaches at least 152 mm (6 in) at any time during the storm event, the historic 50-year storm produces a total flood extent of 14.5 km². By mid-century, when the 10-GCM ensemble median storm magnitude is projected to increase by 13.8%, median total flood extent will increase by 16% to 16.8 km², not including any effect of SLR. By late-century, the 10-GCM ensemble median storm magnitude increase of 36.9% alone will produce a 43% median increase in total flood extent to 20.8 km².

Changes in median flood extent in the upper watershed will be proportionally larger, increasing 36% by mid-century and 75% by late-century (Table 11). Although, for those parts of the upper watershed not affected by SLR, most flooding is relatively short in duration, as shown in Figures 17 and 18. Approximately 85% of short-term (less than 48 hours) flooding in the upper watershed lasts less than 12 hours, with most lasting 1 to 6 hours under the historic storm or mid-century (Scenario A) conditions (Figure 17). Even under late-century conditions (Scenario C), most flooding lasts between 3 to 12 hours (Figure 18). In the upper watershed, data for Scenarios B and D are similar to Scenarios A and C respectively, given the limited impact of SLR upstream.

When changes in 50-year storm magnitude are combined with SLR, there is little compound effect in the upper watershed at 0.6 m (1.9 ft) and 1 m (3.4 ft) SLR, indicating that precipitation change will be the controlling process in the upper watershed until SLR reaches the extreme scenario of 1.6 m (5.2 ft) (Figure 19). In contrast, there are large compound effects in the lower watershed, most prominently at the lower modeled SLR of 0.6 m (1.9 ft). As shown in Table 12, when storms occur on top of 0.6 m (1.9 ft) SLR, flood extents at all storm magnitudes will be an average of 27% larger overall, and 30% larger in the Baylands, than with no SLR. By mid-century, the 10-GCM ensemble median storm combined with 0.6 m (1.9 ft) SLR, will produce a total compound flood extent of 20.6 km², 26% larger than the storm increase alone and 50% larger than SLR alone (Figure 20).

When SLR reaches 1 m (3.4 ft) and above, nearly the entire Baylands will be inundated and SLR becomes the controlling process for both the Baylands and total compound flood extent. SLR of 1 m (3.4 ft) and 1.6 m (5.2 ft) will produce nearly the same flood extent of 22.8 km² and 23.9 km² respectively. When a 50-year storm is combined with these high sea levels, total compound flood extent is only 6% to 16% greater depending on the size of the storm, although nearly all of this increase will impact more densely populated areas upstream. The mid-century 10-GCM ensemble median storm combined with 1 m (3.4 ft) SLR, results in total compound flood extent that is 77% larger than the historic 50-year storm, but only 13% more than 1 m (3.4 ft) SLR alone. Similarly, the

late-century 10-GCM ensemble median storm combined with 1.6 m (5.2 ft) SLR, produces a compound flood extent that is 83% larger than the historic 50-year storm, but only 12% more than 1.6 m (5.2 ft) SLR alone. These compound effects can be seen in Figure 21 which shows that total flood extent will increase 42% to 77% by mid-century under Scenarios A and C, and 82% to 83% by late-century under Scenarios C and D, relative to the historic 50-year storm.

It is important to note that all modeled flood extent results are based on a constant tidal boundary set at MHHW. Actual flooding could reach a somewhat smaller area and/or recede more quickly when the storm peak does not coincide with high tide.

Flood Depth

Maximum flood depth rises continuously with increasing storm magnitude as shown in Figure 22. In addition, because the steep topography of the watershed constrains flood extent as precipitation increases, the area exposed to dangerously deep flood levels can increase proportionally more than flood extent overall. For example, the maximum total extent of flooding caused by the 10-GCM ensemble median storm (with no SLR) is approximately 17% larger than that of the historic 50-year storm. But for this same change in storm magnitude, the area covered by 0.3 to 0.6 m (1 to 2 ft) of water increases 50% and the area covered by 1.2 to 1.8 m (4 to 6 ft) of water increases 150%. If storm

magnitude were to increase to the level of the highest GCM projection (53%) for mid-century, the area covered by 0.3 to 0.6 m (1 to 2 ft) of water would double relative to the historic storm and the area flooded by 1.2 to 1.8 m (4 to 6 ft) would almost triple.

With the addition of SLR, there are large compound effects on flood depth as indicated by the rightward shift of the peaks of the flooded area distributions in Figure 23. Not surprisingly, the depth distributions shift significantly under every compound climate change scenario as compared to the historic 50-year storm. The area subject to flooding also increases substantially at every depth for compound Scenario A, as compared to 0.6 m (1.9 ft) SLR alone. At higher SLR, the depth distributions for both SLR alone and compound flood scenarios are dominated by the increases in depths greater than 2.4 m (8 feet) due to SLR effects in the Baylands. This obscures important changes in the heavily populated upper watershed where flood depths over 0.15 m (0.5 ft) could pose significant danger to people and infrastructure. As shown in Figure 24, under Scenario A in the upper watershed, 38% more area is flooded 0.3 to 0.6 m (1 to 2 ft) and 52% more area is flooded 0.6 to 0.9 m (2 to 3 ft) compared to the historic storm. Under Scenario C, these increases are 73% for flood depth of 0.3 to 0.6 m (1 to 2 ft) and 129% for flood depth of 0.6 to 0.9 m (2 to 3 ft). This deeper flooding is also likely to last at least a few hours longer given the shifts in flood duration described earlier (Figure 17).

Socio-Economic Impacts and Vulnerability

Population and Social Vulnerability

According to estimates from the 2016 American Community Survey (U.S. Census Bureau, 2019), there are 62,176 people living in the Novato CCD, which includes the City of Novato and surrounding unincorporated communities mostly lying within the Novato Creek watershed. As shown in Table 13, the Novato CCD comprises 24% of the total population of Marin County, and within the Novato CCD, 18% of the population is age 65 or older, 8% have income below 100% of the FPL, and 21% have income below 200% of the FPL. These proportions of vulnerable populations are similar to their share in the county as a whole, with slightly greater share of low-income people in Novato. Under current climate conditions, a 50-year flood will impact almost 6,500 people, approximately 10% of the population within the Novato CCD. Under future compound flood scenarios, this total will rise by 46% to 78%, with nearly 11,500 people impacted under Scenario D, representing 18% of the total population. Further, these figures do not include possible future growth in the local population from now to 2100, and therefore probably represent minimum future impacts absent significant changes in housing and commercial development or flood control measures.

Vulnerable older and low-income population groups will be impacted by flooding in relatively similar proportion to their representation in the local population overall. Across

all current and future flood scenarios, 15% of people in the flood zone will be age 65 or over, as compared to 18% within the Novato CCD population as a whole. Very poor people, with incomes below 100% of the FPL, will comprise 8% of the people impacted by future flooding, the same proportion as their representation in the total population. Approximately 25% of the larger portion of low-income people with incomes up to 200% of the FPL will be impacted by future flooding, a small increase over their 21% representation in the total Novato CCD population. However, lower-income people may be more disproportionately impacted by deeper and longer duration flooding given their concentration in lower elevation areas of the upper watershed. The location of low-income populations relative to modeled mid- and late-century flood zones is shown in Figure 25.

Roads

Road projections may somewhat overestimate impacts because the road data contained fire roads, service roads, driveways, walkways, and railroad access roads that may not be core to local mobility. However, impacts will be significant under all climate change scenarios. Figure 26 shows the lengths of all roads and major highways that are projected to be flooded at any time by at least 152 mm (6 in) of water under Scenarios A – D, the historic 50-year storm, and SLR alone. Impacts range from a more than 60% increase in total road miles flooded under Scenario A as compared to the historic 50-year storm, to a 170% increase in Scenario D. The region's major highways will be similarly highly

impacted, especially CA-37. By mid-century under Scenario A, a 50-year storm will flood 1.9 more miles of major roads, a 50% increase over the historic storm. Under Scenario B, with 1 m (3.4 ft) SLR by mid-century, 3.3 miles of major roads could be permanently inundated or regularly flooded by high tides, and an additional 4.6 miles could flood during a storm event. Under late-century scenarios, SLR could inundate 3.3 to 4.6 miles of major roads, and a storm event would flood an additional 5 to 6 miles.

Residential and Commercial Property

Climate change will cause even greater proportional increases in flood impacts to property in the Novato Creek watershed. Model results show that during the historic 50-year storm, flood waters can reach 1156 residential buildings, 326 commercial/industrial buildings, and 33 other non-residential properties. By mid-century, impacted residential buildings will increase by 72% and 99% under Scenarios A and B. By late-century, residential impacts will more than double under Scenarios C or D (Figure 27). Most of these impacts will occur in the upper watershed where residential development is concentrated (Figure 28). Although depth and duration analyses (Figures 17 and 24) show that flood depths are likely to be relatively low and recede in less than 6 to 12 hours in much of the upper watershed, such flooding could still cause substantial property damage. In the Baylands, hundreds of properties, mostly in the Bel Marin Keys neighborhood, could be permanently inundated or regularly flooded at high tide due to

SLR. However, existing tide gates and plans to increase sea walls could hold off such flooding until extreme sea levels are reached.

Critical Facilities

Table 14 shows that no police, fire or major hospital facilities will be directly exposed to flooding under any of the climate scenarios investigated in this study. Two power substations and a community center in the Bel Marin Keys area are vulnerable to SLR. Under the most extreme conditions modeled, Scenario D, four educational facilities, one home health care center, the North Marin Water District Office, plus the two power substations and Bel Marin Keys Community Center, will be directly exposed to flooding. However, these numbers underestimate critical facility impacts, as additional facilities (e.g., Marin Community Hospital, Novato Fire Protection District Office) may be inaccessible under mid- or late-century conditions due to flooding of surrounding roads. Figure 28 shows where critical facilities are located relative to flooding under Scenarios A and C.

CONCLUSION

Climate change will affect both fluvial and coastal flooding, yet few studies have modeled the compound effects of these distinct physical processes. In this study, I found that by key measures – channel discharge, flood extent, flood depth and socio-economic impacts – compound effects on flooding differ significantly from analysis of changes in fluvial or SLR processes alone. The Novato Creek watershed demonstrates the impacts of compound flooding in a location where steep topography creates a distinct boundary on the upstream influence of SLR. As a result of this topography, for storms with a 50-year return period, changes in precipitation control flooding upstream of areas where elevation is higher than projected sea level. Downstream, SLR controls flooding when sea level is high enough to inundate most low-lying area. Compound effects are greatest in the range where neither SLR nor storm precipitation alone can fully inundate the lower watershed.

In the Novato Creek watershed, the 10 GCMs used in this study project that future 50-year storms could change by -7% to 68% during this century, with multimodel ensemble median changes of 13.8% by mid-century (2040-69) and 36.9% by late-century (2070-2099). With these increases, by mid-century a 50-year storm will be larger than today's 100-year storm, and by late-century a 50-year storm will be larger than today's 200-year storm.

The intermediate to high risk SLR projections selected for this study are 0.6 m (1.9 ft) for mid-century (2040-2069) and 1 m (3.5 ft) by late-century (2070-2099), with an extreme scenario of 1.6 m (5.2 ft) by 2070. When the ensemble median projected changes in precipitation were modeled in combination with these SLR projections, total flood extent in the Novato Creek watershed showed projected increases over the historic 50-year storm of 42% to 77% by mid-century and 82% to 83% by late-century. Flood depths and durations will also increase significantly.

The socio-economic impacts of these compound effects of climate change are many multiples greater than from SLR alone, given that effects extend into the densely populated upper watershed. While the permanent inundation caused by SLR is more severe than the relatively short-term flooding caused by storms, compound flooding will exceed 0.3 m (1 ft) depth and 3 or more hours in most places, causing substantial disruption and damage in large areas not directly affected by SLR. The total number of people impacted by flooding will increase from 6,500 under historic storm conditions, to at least 9,400 by mid-century and 11,400 by late-century. Vulnerable populations of low-income and older residents will be impacted in large numbers, but not disproportionate to their presence in the total population. Although it is possible those low-income people who are impacted could experience relatively longer and deeper flooding given their

concentration in lower elevation areas of the upper watershed. The length of roads impacted by flooding will increase 60% to 170% over the 32 km (20 miles) flooded by the historic storm, including 8 to 16 km (5 to 10 miles) of lanes of US 101, CA-37, and other major roads. Thousands of additional homes and other buildings will also be exposed to flooding due to climate change, increasing 60% to 115% over the 1515 buildings exposed to flooding by the historic 50-year storm, although no emergency services and very few other critical facilities will be directly impacted by flood waters.

The scale of these projected impacts makes clear the importance of considering compound flood effects when planning for climate change adaptation. Further analysis could explore additional socio-economic indicators and breakdown impacts by the depth and duration of flood exposure. More importantly, future research should focus more directly on thresholds for critical harm (e.g., when levees will overtop or essential roads and bridges will be flooded) and joint probabilities of compound flood events, working backwards to determine the various combinations of climate changes that could trigger flooding over such thresholds. Additional advanced research could also seek to incorporate a variable tidal boundary, changes in lower watershed geometry and intertidal flows that might occur as sea level rises, or other dynamic factors, such as potential changes in landcover or population density, in the model design.

TABLES

Table 1: Climate change scenarios used to investigate changes in flood hazard and socio-economic impacts of compound flooding. All scenarios are for 50-year (2% annual chance of occurrence) storms.

Climate Change Scenarios			
Scenario #	Time Period	RCP 8.5 Median Precipitation Change (%)	Sea Level Rise (m/ft)
A	Mid-Century (2040-69)	13.8	0.6 m / 1.9 ft
B	Mid-Century (2040-69)	13.8	1.0 m / 3.4 ft
C	Late-Century (2070-99)	37.0	1.0 m / 3.4 ft
D	Late-Century (2070-99)	37.0	1.6 m / 5.2 ft

Table 2: “California GCMs” recommended by California Dept. of Water Resources for climate modeling for California. (DWR, 2015; Pierce et al., 2018)

“California GCMs” Recommended by CA Dept. of Water Resources	
Model Name	Source Institution
ACCESS-1.0	Commonwealth Scientific and Industrial Research Organization (CSIRO) and Bureau of Meteorology, Australia
CCSM4	National Center for Atmospheric Research (NCAR)
CESM1-BGC	The National Science Foundation, The U.S. Department of Energy, and National Center for Atmospheric Research
CMCC-CMS	Centro Euro-Mediterraneo per i Cambiamenti Climatici, Italy
CNRM-CM5*	Centre National de Recherches Meteorologiques (CNRM), and Centre Europeen de Recherches et de Formation Avancee en Calcul Scientifique, France
CanESM2*	Canadian Centre for Climate Modeling and Analysis
GFDL-CM3	Geophysical Fluid Dynamics Laboratory, National Oceanic and Atmospheric Administration (NOAA)
HadGEM2-CC	Met Office Hadley Centre
HadGEM2-ES*	Met Office Hadley Centre (additional HadGEM2-ES realizations contributed by Instituto Nacional de Pesquisas Espaciais)
MIROC5*	Atmosphere and Ocean Research Institute, University of Tokyo, National Institute for Environmental Studies, and Japan Agency for Marine-Earth Science and Technology

*subset of 4 GCMs recommended when a project doesn’t have resources to process all 10 GCMs.

Table 3: Projected two-day, 50-year storm magnitudes under RCP 4.5 for Novato Creek (LOCA cell# 6434) for each California GCM for three future time periods, with percentage change over historic period (1950-2005).

48-Hr 50-Yr Storm Magnitude, RCP 4.5 (mm)							
California GCMs	1950-2005	2006-2039	% Change	2040-2069	% Change	2070-2099	% Change
ACCESS1-0	221	216	-2.3	290	31.4	268	21.3
CanESM2	223	271	21.0	340	52.0	323	44.7
CCSM4.6	234	243	3.9	237	1.3	212	-9.3
CESM1-BGC	228	299	31.0	261	14.5	252	10.4
CNRM-CM5	217	335	54.4	334	53.8	292	34.7
GFDL-CM3	231	185	-19.8	269	16.3	214	-7.3
CMCC-CMS	234	198	-15.3	262	12.3	329	41.0
HadGEM2-CC	228	232	1.9	266	16.5	220	-3.4
HadGEM2-ES	231	202	-12.8	258	11.6	279	20.5
MIROC5	225	231	2.8	248	10.5	254	12.8
Ensemble median	228	232	1.6	264	15.7	261	14.3
Ensemble mean	227 ± 2	241 ± 15	6.1 ± 6.7	276 ± 11	21.7 ± 4.9	264 ± 13	16.4 ± 6.0

Table 4: Projected two-day, 50-year storm magnitudes under RCP 8.5 for Novato Creek (LOCA cell# 6434) for each California GCM for three future time periods, with percentage change over historic period (1950-2005).

48-Hr 50-Yr Storm Magnitude, RCP 8.5 (mm)							
California GCMs	1950-2005	2006-2039	% Change	2040-2069	% Change	2070-2099	% Change
ACCESS1-0	221	234	5.7	245	10.8	305	38.0
CanESM2	223	264	18.3	343	53.4	355	58.7
CCSM4.6	233	235	0.7	224	-3.9	264	13.3
CESM1-BGC	228	322	41.2	303	32.8	241	5.7
CNRM-CM5	218	322	47.8	298	37.0	366	68.1
GFDL-CM3	231	198	-14.5	226	-2.1	234	1.1
CMCC-CMS	233	233	-0.1	274	17.6	347	48.9
HadGEM2-CC	228	221	-3.2	241	5.7	326	42.7
HadGEM2-ES	231	235	1.6	274	18.6	319	38.2
MIROC5	224	226	1.0	210	-6.4	208	-7.4
Ensemble median	228	234	2.7	259	13.8	312	36.9
Ensemble mean	227 ± 2	249 ± 13	9.6 ± 5.9	264 ± 13	16.2 ± 5.9	296 ± 18	30.5 ± 7.8

Table 5: Projected two-day, 100-year storm magnitudes under RCP 4.5 for Novato Creek (LOCA cell# 6434) for each California GCM for three future time periods, with percentage change over historic period (1950-2005).

48-Hr 100-Yr Storm Magnitude, RCP 4.5 (mm)							
California GCMs	1950-2005	2006-2039	% Change	2040-2069	% Change	2070-2099	% Change
ACCESS1-0	245	239	-2.2	323	31.7	295	20.3
CanESM2	247	301	22.1	381	54.5	359	45.5
CCSM4.6	259	270	4.3	262	1.1	233	-10.0
CESM1-BGC	252	333	31.7	290	14.8	280	10.9
CNRM-CM5	240	371	54.8	371	54.7	323	34.8
GFDL-CM3	255	202	-20.8	298	16.7	232	-9.1
CMCC-CMS	259	216	-16.4	292	12.7	368	42.0
HadGEM2-CC	251	259	2.9	296	17.6	243	-3.4
HadGEM2-ES	257	221	-13.9	286	11.6	308	20.2
MIROC5	249	256	2.6	276	10.7	282	13.1
Ensemble median	252	257	2.1	294	16.6	288	14.4
Ensemble mean	251 ± 2	267 ± 17	6.1 ± 6.8	307 ± 13	22.3 ± 5.0	292 ± 15	16.3 ± 6.2

Table 6: Projected two-day, 100-year storm magnitudes under RCP 8.5 for Novato Creek (LOCA cell# 6434) for each California GCM for three future time periods, with percentage change over historic period (1950-2005).

48-Hr 100-Yr Storm Magnitude, RCP 8.5 (mm)							
California GCMs	1950-2005	2006-2039	% Change	2040-2069	% Change	2070-2099	% Change
ACCESS1-0	245	258	5.4	271	10.5	340	38.9
CanESM2	247	293	18.6	384	55.5	393	59.1
CCSM4.6	258	260	1.0	246	-4.5	291	12.9
CESM1-BGC	252	359	42.6	337	33.7	263	4.5
CNRM-CM5	240	358	49.1	331	37.5	407	69.2
GFDL-CM3	255	216	-15.3	248	-3.0	255	0.0
CMCC-CMS	258	255	-1.2	305	18.0	389	50.7
HadGEM2-CC	252	244	-2.9	267	6.0	366	45.1
HadGEM2-ES	257	260	1.2	307	19.7	351	36.6
MIROC5	248	251	1.2	231	-7.0	228	-8.4
Ensemble median	252	259	2.7	288	14.2	345	37.1
Ensemble mean	251 ± 2	276 ± 15	9.7 ± 6.0	293 ± 15	16.5 ± 6.2	328 ± 20	30.6 ± 8.1

Table 7: Probabilistic sea level rise projections under RCP 8.5 emissions scenario, from (Kopp et al., 2014; OPC, 2018) (white/no shading) and (NOAA, 2018; Sweet et al., 2017) (gray shading).

Projected Sea Level Rise at San Francisco, CA (feet)					
Year	Intermediate Low	Intermediate	Intermediate High	High	Extreme
	Median – 50% probability	Likely Range 66% probability	1-in-20 chance, 5% probability	1-in-200 chance, 0.5% probability	(no probability assigned)
2040	0.6	0.5 – 0.8	1.0	1.3	1.8
	0.56	0.82	1.12	1.51	1.77
2050	0.9	0.6 – 1.1	1.4	1.9	2.7
	0.72	1.18	1.67	2.30	2.72
2060	1.1	0.8 – 1.5	1.8	2.6	3.9
	0.92	1.54	2.26	3.18	3.87
2070	1.4	1.0 – 1.9	2.4	3.5	5.2
	1.08	1.94	2.95	4.17	5.18
2080	1.7	1.2 – 2.4	3.0	4.5	6.6
	1.25	2.40	3.74	5.35	6.63
2090	2.1	1.4 – 2.9	3.6	5.6	8.3
	1.41	2.85	4.63	6.69	8.27
2100	2.5	1.6 – 3.4	4.4	6.9	10.2
	1.57	3.41	5.71	8.30	10.20

Table 8: Socio-economic impact indicators and GIS data sources.

Socio-Economic Impact Indicators and GIS Data Sources		
Indicator	Description	Data Source
POPULATION		
Total population	Count of total population by census block group.	U.S. Census Bureau, TIGER/Line Shapefiles with 2012-2016 American Community Survey 5-Year Estimates by Census Block Group.
Age 65 and over	Count of all men and women age 65 or older by census block group.	
Poverty: <100% of FPL	Count of all individuals with ratio of income to poverty level 0.99 and under in the past twelve months, by census block group.	
Poverty: < 200% of FPL	Count of all individuals with ratio of income to poverty level 1.99 and under in the past twelve months, by census block group.	
TRANSPORTATION		
Roads	Line representation of vehicle and pedestrian access ways in Marin County. Includes roads, fire roads, service roads, driveways, trails, walkways, railroad lines and docks. The GIS feature class was originally created from a query of the Census TIGER file for these access types. Entities were edited to align to visible features on the 2004 Marin County digital Orthophoto.	MarinMap, a Geographic Information System for Marin County, California, www.marinmap.org
Major roads	Major roads are a subset of the Roads data, limited to interstate and state highways, major local thoroughfares and their onramps and access roads.	
Bridges	Point location of bridges from the National Bridge Inventory. It contains bridges located on public roads, including interstate highways, U.S. highways, state and county roads, as well as publicly-accessible bridges on Federal lands.	
FACILITIES		
Building footprints	Building footprint outlines produced using stereo pairs from the Marin County 2004 orthophoto high-resolution aerial photography. Buildings are categorized into 13 types, including residential, commercial, industrial, medical, education, etc.	MarinMap, a Geographic Information System for Marin County, California, www.marinmap.org
Critical Facilities	Point locations of the following types of facilities: <ul style="list-style-type: none"> • Emergency services, including police, fire stations, and City Hall • Hospitals & medical centers, including clinics and mental health services • Schools & community centers, including child care centers • Utilities, consisting of wastewater treatment plants and power substations 	

Table 9: Projected changes in two-day storm magnitude based on RCP 8.5 10-GCM ensemble mean change factors, compared to historic storm magnitudes and frequencies.

Novato Creek Watershed, 2-Day Storm Magnitude (mm)			
Return Period	Atlas-14 Historic	GCM Projection 2040-69	GCM Projection 2070-99
50 years (2 %)	211	245 ± 13	275 ± 17
100 years (1%)	236	275 ± 14	308 ± 19
200 years (0.5%)	260		
500 years (0.2%)	294		

Table 10: Peak discharge in Novato Creek at selected upstream and downstream cross-sections under different climate change scenarios. Precipitations changes are for 48-hour, 50-year storm under historic conditions and RCP 8.5. Upstream discharge measured at HEC-RAS RS 39926 near the USGS stream gage. Downstream discharge measured at RS 32080 in the lower creek below the confluence of Arroyo Avichi and the main channel.

Peak Discharge by Change in Precipitation and SLR									
48-Hr, 50-Yr Storm, RCP 8.5									
GCM	Precipitation Change (%)	Upstream Discharge by SLR (cfs)				Downstream Discharge by SLR (cfs)			
		None	1.9 ft	3.4 ft	5.2 ft	None	1.9 ft	3.4 ft	5.2 ft
Historic Storm	0%	3052	3051	3051	3052	4702	4701	4700	4701
MIROC5	-6.4%	2986	2986		2986	4508	4507		4497
CCSM4.6	-3.9%	3010				4586			
GFDL-CM3	-2.1%	3023				4640			
HadGEM2-CC	5.7%	3583				4929			
ACCESS1-0	10.8%	3580	3580			5128	5126		
CMCC-CMS	17.6%	3676				5438			
HadGEM2-ES	18.6%	3684	3685		3684	5498	5484		5463
CESM1-BGC	32.8%	3809	3809			6047	6046		
CNRM-CM5*	37.0%	3838	3838	3837	3837	6194	6193	6189	6182
CanESM2	53.4%	3965	3965		3965	6639	6635		6624
Ensemble median	13.8%		3625	3625			5269	5263	

*Results from modeling of CNRM-CM5 also used as proxy for late-century 10-GCM ensemble median.

Table 11: Modeled changes in flood extent due to mid-century (2040-69) RCP 8.5 precipitation change projections for 10 California GCMs with no change in SLR. All changes are relative to the historic (1950-2005) 50-year storm. Flood extent is maximum area covered by at least 152mm (6 in) of water at any time during the storm.

Maximum Flood Extent by Change in Precipitation 48-Hr, 50-Yr Storm, RCP 8.5, No SLR							
Global Climate Model (GCM)	Precipitation % change	Maximum Flood Extent					
		Total Watershed		Upper Watershed		Lower Watershed	
		km ²	% change	km ²	% change	km ²	% change
Historic 50-yr Storm		14.50		1.73		12.77	
MIROC5	-6.4	13.83	-4.6	1.40	-19.1	12.43	-2.7
CCSM4.6	-3.9	14.10	-2.8	1.53	-11.6	12.57	-1.6
GFDL-CM3	-2.1	14.32	-1.2	1.62	-6.4	12.70	-0.5
HadGEM2-CC	5.7	15.47	6.7	1.98	14.5	13.49	5.6
ACCESS1-0	10.8	16.22	11.9	2.22	28.3	14.00	9.6
CMCC-CMS	17.6	17.40	20.0	2.49	43.9	14.91	16.8
HadGEM2-ES	18.6	17.47	20.5	2.51	45.1	14.96	17.1
CESM1-BGC	32.8	20.21	39.4	2.94	69.9	17.27	35.2
CNRM-CM5*	37.0	20.79	43.4	3.04	75.7	17.75	39.0
CanESM2	53.4	22.40	54.5	3.38	95.4	19.02	48.9
Ensemble Median	13.8	16.83	16.1	2.36	36.4	14.47	13.3

*Results from modeling of CNRM-CM5 also used as proxy for late-century 10-GCM ensemble median.

Table 12: Modeled change in flood extent due to mid-century (2040-69) RCP 8.5 precipitation change projections for subset of four California GCMs plus SLR projections. All changes relative to historic 50-year storm with no SLR. Empty areas of table indicate model not run for that scenario.

Maximum Flood Extent by Change in Precipitation and SLR									
48-Hr, 50-Yr Storm, RCP 8.5									
Storm/GCM	Precipitation (% change)	Maximum Flood Extent (152mm (6 in) < depth)							
		No SLR		0.6 m (1.9 ft) SLR		1 m (3.4 ft) SLR		1.6 m (5.2 ft) SLR	
		km ²	% chg	km ²	% chg	km ²	% chg	km ²	% chg
Historic 50-yr Storm		14.50		18.44	27.2	25.11	73.2	25.57	76.3
Upper Watershed	0.0	1.73		1.83	5.8	1.98	14.5	2.19	26.6
Lower Watershed		12.77		16.61	30.1	23.13	81.1	23.38	83.1
No Storm, SLR only				13.71		22.82		23.85	
Upper Watershed	0.0			0.00		0.14		0.58	
Lower Watershed				13.71		22.68		23.27	
MIROC5		13.83	-4.6	17.83	23.0			25.33	74.7
Upper Watershed	-6.4	1.40	-19.1	1.51	-12.7			1.96	13.3
Lower Watershed		12.43	-2.7	16.32	27.8			23.37	83.0
HadGEM2-ES		17.47	20.5	21.39	47.5			26.14	80.3
Upper Watershed	18.6	2.51	45.1	2.56	48.0			2.72	57.2
Lower Watershed		14.96	17.1	18.83	47.5			23.42	83.4
CNRM-CM5*		20.79	43.4	24.57	69.4	26.38	81.9	26.60	83.4
Upper Watershed	37.0	3.04	75.7	3.06	76.9	3.09	78.6	3.15	82.1
Lower Watershed		17.75	39.0	21.51	68.4	23.29	82.4	23.45	83.6
CanESM2		22.40	54.5	25.65	76.9			26.94	85.8
Upper Watershed	53.4	3.38	95.4	3.40	96.5			3.45	99.4
Lower Watershed		19.02	48.9	22.25	74.2			23.49	83.9
Mid-Century Median		16.83	16.1	20.60	42.1	25.68	77.1		
Upper Watershed	13.8	2.36	36.4	2.40	38.7	2.48	43.4		
Lower Watershed		14.47	13.3	18.20	42.5	23.20	81.7		

*Results from modeling of CNRM-CM5 also used as proxy for late-century 10-GCM ensemble median

Table 13: Total population and socially vulnerable populations exposed to flooding from two-day, 50-year storm under different compound flood scenarios.

Populations Exposed to Flooding								
	Total Population		Population in Flooded Areas					
			Age 65 and over		Income below poverty line			
	Total	%	65<=	%	< 100%	%	< 200%	%
Total Population								
Marin County	259,358	100%	50,575	20%	19,762	8%	46,648	18%
Novato CCD	62,176	24%	11,297	18%	4,902	8%	13,138	21%
Climate Scenario								
Historic storm	6,454	10%	976	15%	576	9%	1,843	29%
Scenario A	9,419	15%	1,420	15%	773	8%	2,369	25%
Scenario B	10,176	16%	1,553	15%	823	8%	2,482	24%
Scenario C	11,403	18%	1,741	15%	930	8%	2,842	25%
Scenario D	11,501	18%	1,756	15%	938	8%	2,867	25%

Table 14: Critical facilities exposed to flooding from two-day, 50-year storm under different climate change and compound flood scenarios.

Critical Facilities Exposed to Flooding				
Scenario	Emergency Services	Hospitals & Medical Centers	Schools & Community Centers	Utilities
SLR 1.9 ft	0	0	0	1
SLR 3.4 ft	0	0	0	2
SLR 5.2 ft	0	0	0	2
Historic storm	0	1	3	2
Scenario A	0	1	3	3
Scenario B	0	1	3	3
Scenario C	0	1	4	3
Scenario D	0	1	4	3

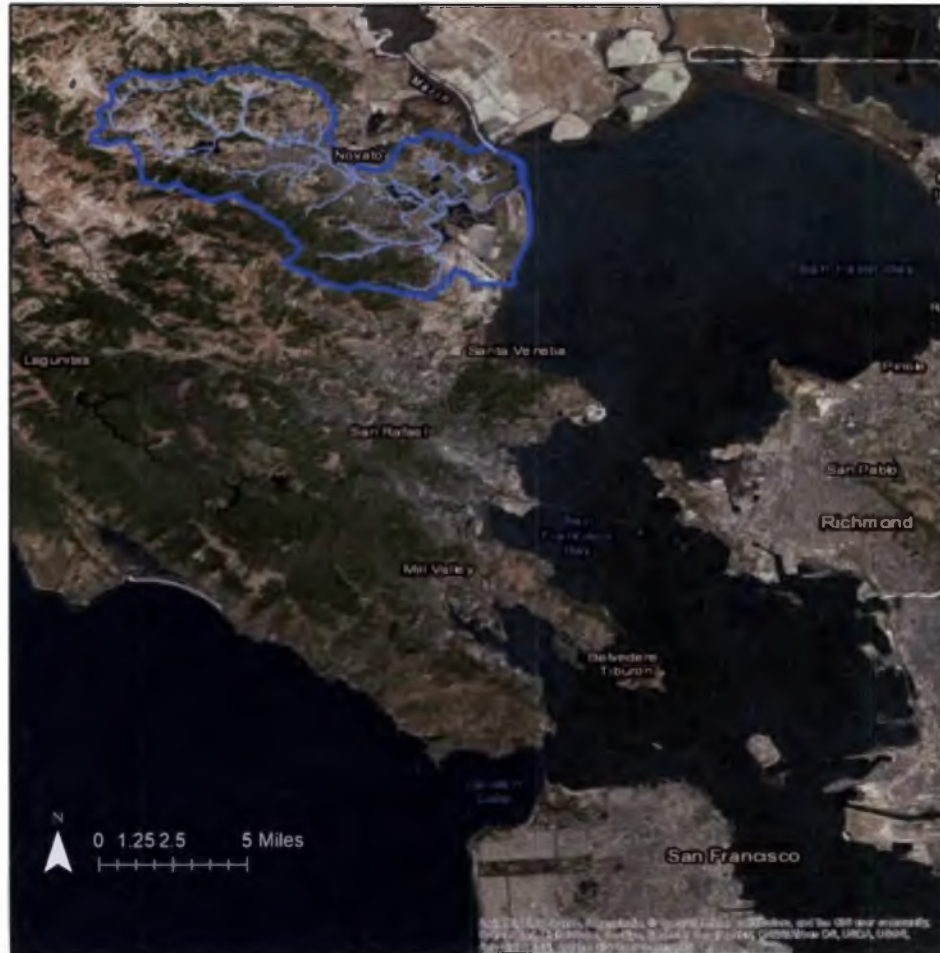
FIGURES

Figure 1: Map of San Francisco Bay showing location of Novato Creek watershed in Marin County north of the City of San Francisco.

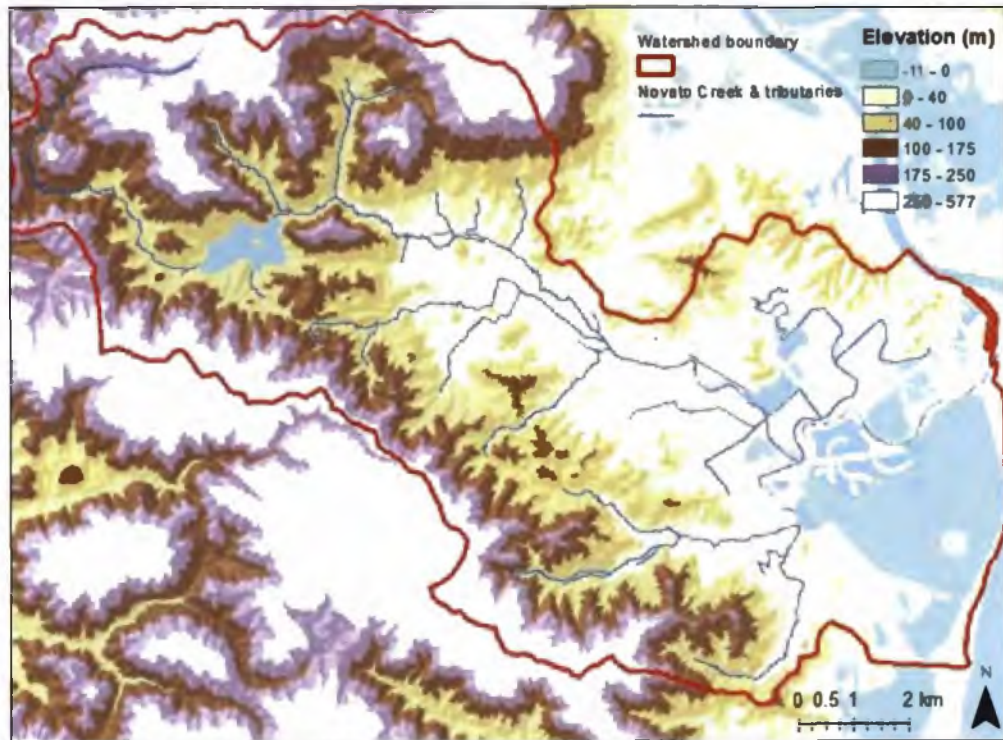


Figure 2: Elevation map of Novato Creek watershed.

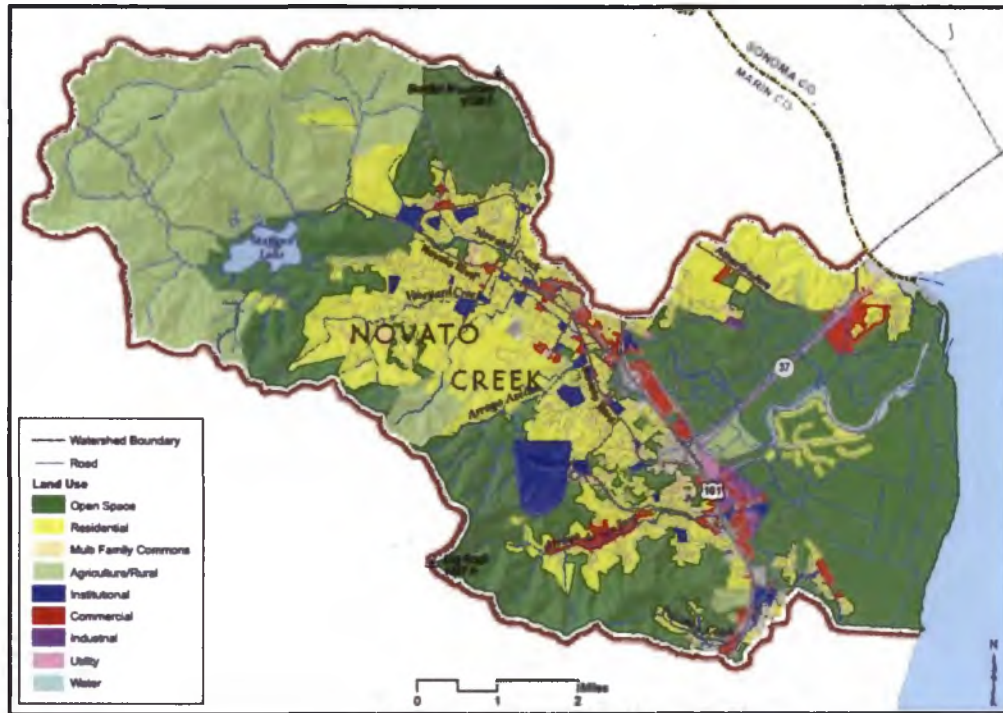


Figure 3: Types of land use within Novato Creek watershed (Source: Marin County Dept. of Public Works).

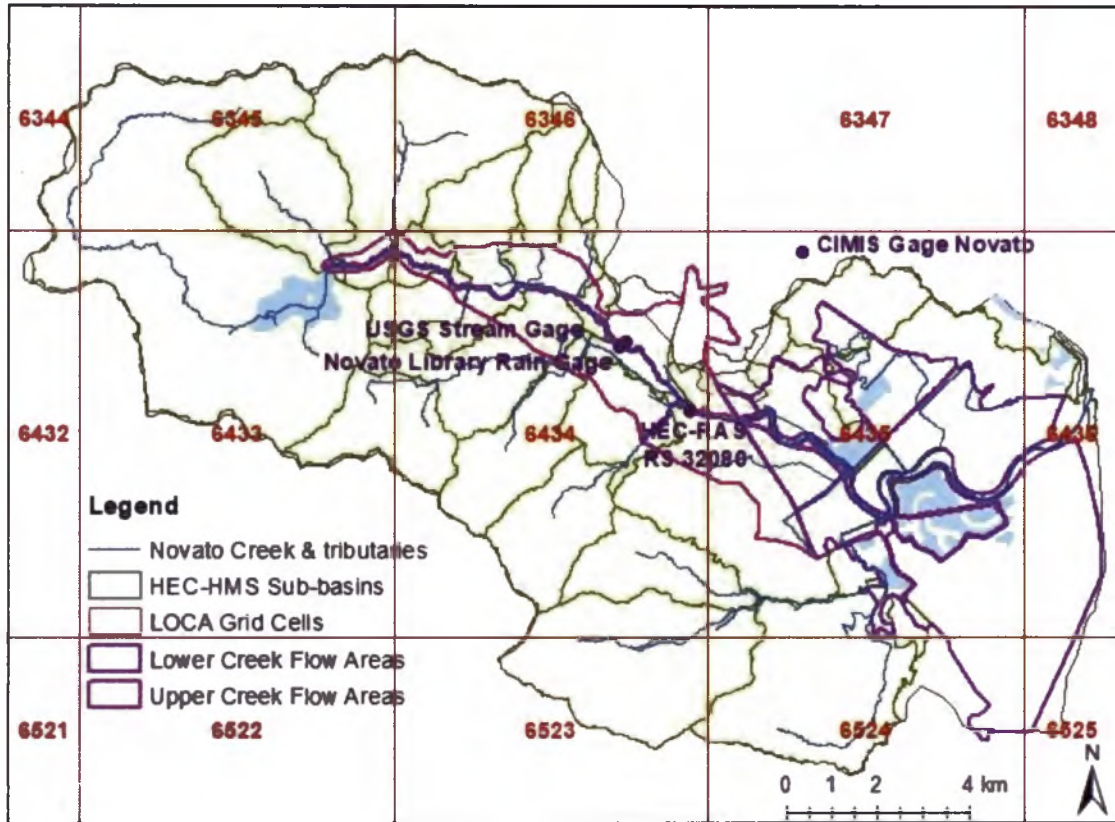


Figure 4: Outline of Novato Creek watershed and stream channels, showing boundaries of 1/16 degree LOCA downscaling grid and cell numbers (red lines and numbers), sub-basins used in HEC-HMS hydrologic model (dark green lines), HEC-RAS 2D flow areas for the Upper Creek (pink lines) and Lower Creek/Baylands (purple lines), and locations of weather stations, stream gages, and channel discharge measurement locations (dots).

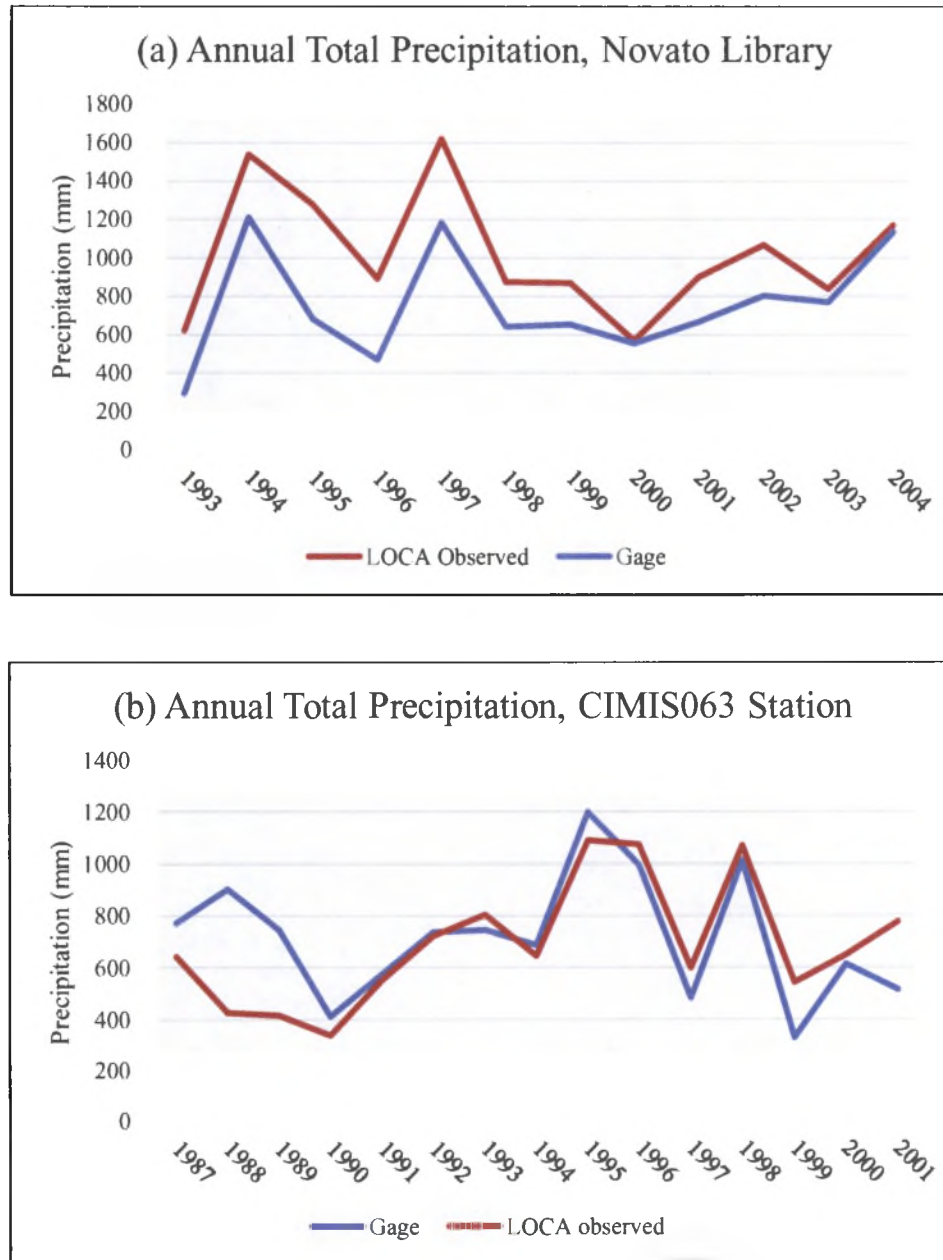


Figure 5: Comparison of gridded LOCA observed data vs. total annual precipitation from weather station point observations for corresponding periods of record at locations of (a) Novato Library county rain gage ($X^2 = 3.85, p = 0.05$) and (b) CIMIS station 063 ($X^2 = 0.05, p = 0.82$).

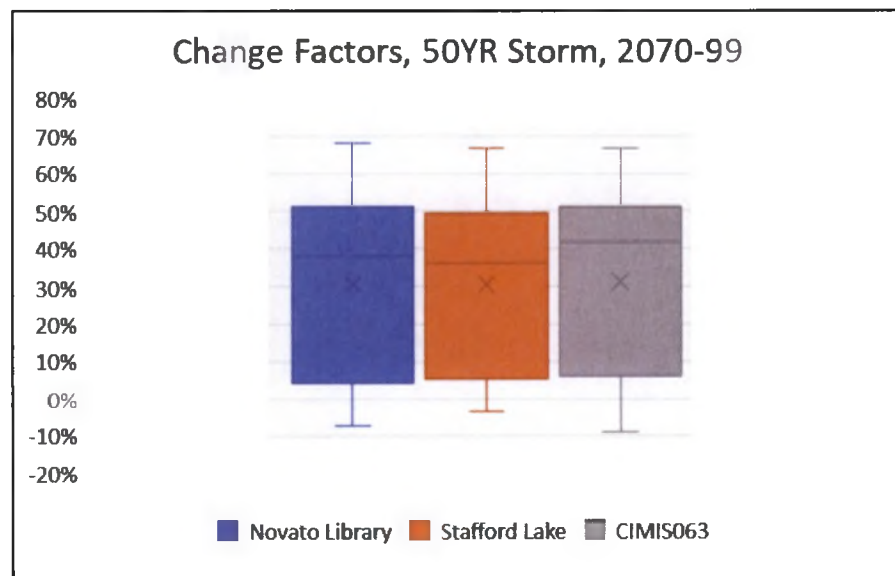
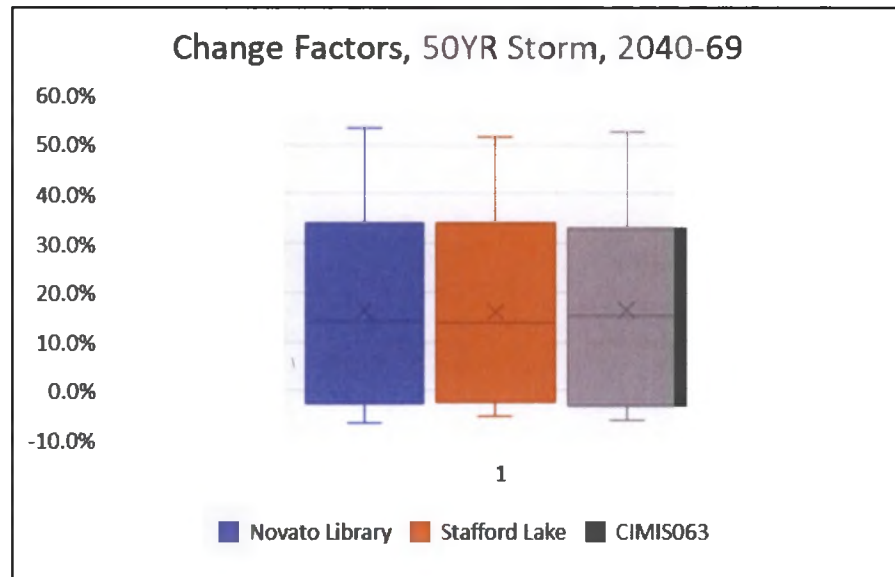


Figure 6: Distribution of change factors for two-day 50-year storm from 10 California GCMs for three LOCA downscaling grid cells. Novato Library (cell# 6434) is located in the center, CIMIS063 (cell# 6435) is on the northeastern edge, and Stafford Lake (cell# 6345) is in the northwestern corner of the Novato Creek watershed. Wilcoxon test indicates there are not significant differences among locations ($X^2 = 0.0045$, $p = 0.998$, $\alpha = 0.05$).



Figure 7: Map of inundation extents (additive for each increase) for 21st Century sea level rise projections for Novato Creek watershed, relative to major highways and populated areas. Source: Modeled study results for areas within the HEC-RAS model extent, and Our Coast Our Future (Ballard et al., 2016) for adjacent areas.

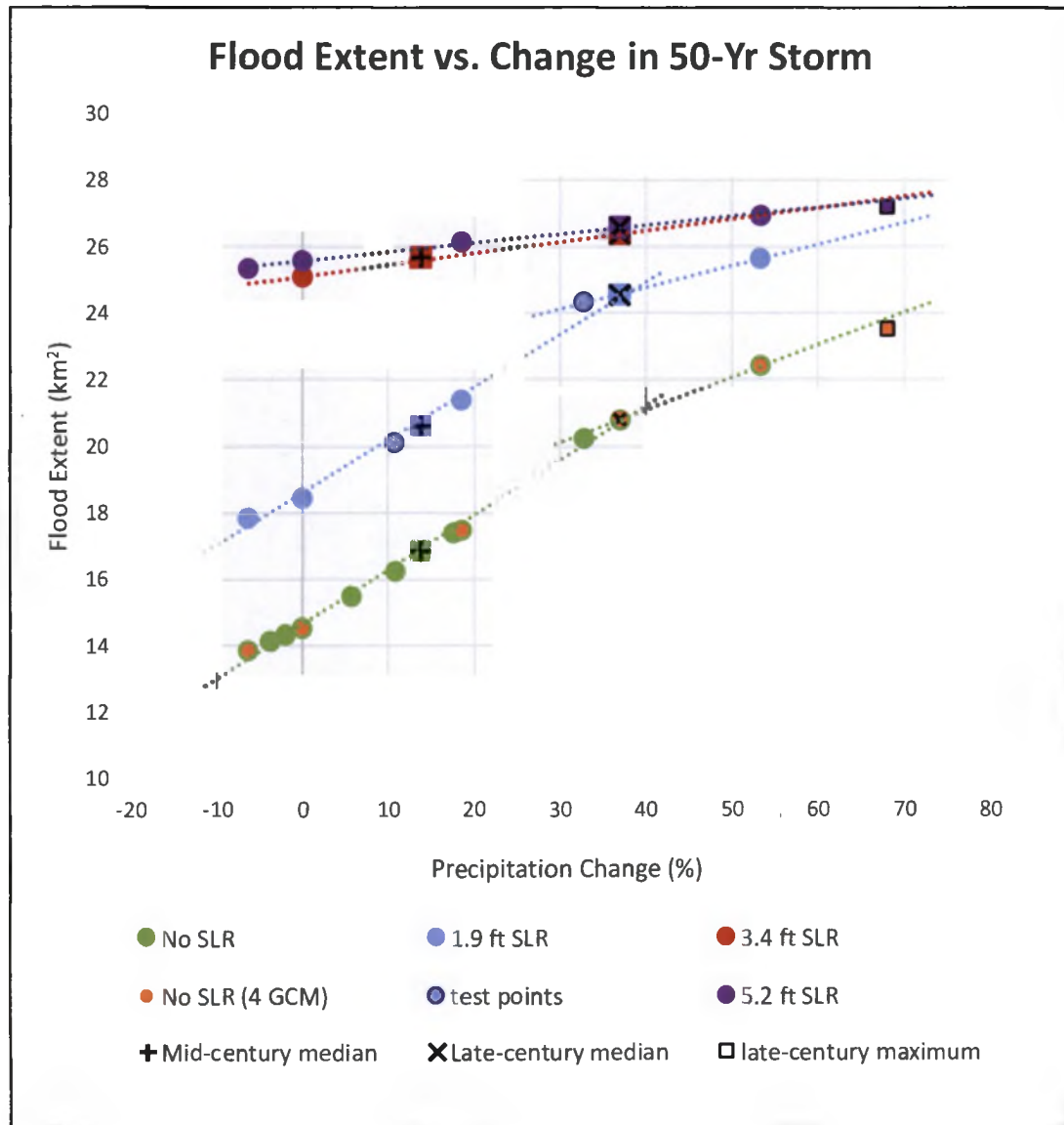


Figure 8: Flood extent for all modeled combinations of precipitation change and SLR for two-day, 50-year storm under RCP 8.5. Dotted lines are plotted using results for historic storm and 10 California GCMs with no SLR, plus historic storm and subset of 4 California GCMs for SLR of 1.9 ft and 5.2 ft. Other points were plotted independently and confirm linear pattern of relationship between increases in precipitation and flood extent.

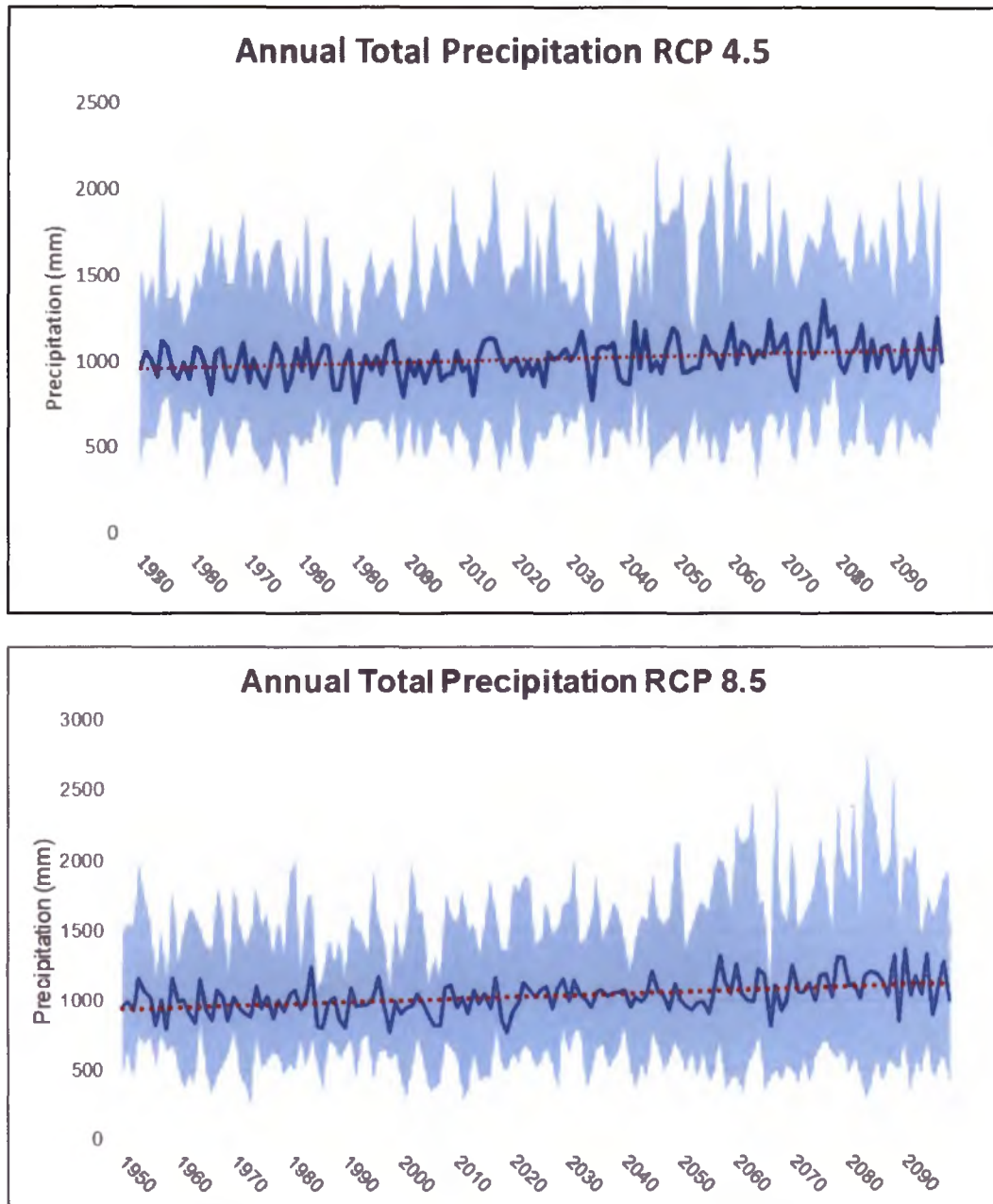


Figure 9: Time series of annual total rainfall 1950-2100 under RCP 4.5 and RCP 8.5, showing range of values (blue shaded area), 10-GCM ensemble means (dark blue line) and increasing linear trend (red dotted line).

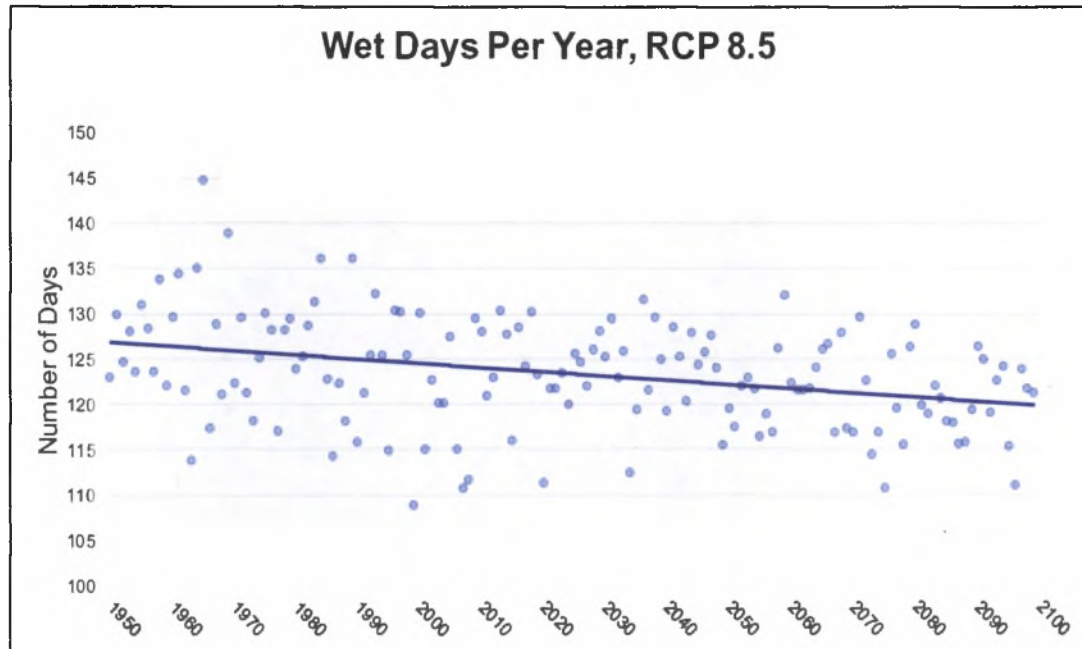


Figure 10: Time series of number of wet days per year, 1950-2100. Data shows RCP 8.5 10-GCM ensemble mean projections for number of days per year with precipitation greater than zero, plus decreasing linear trend.

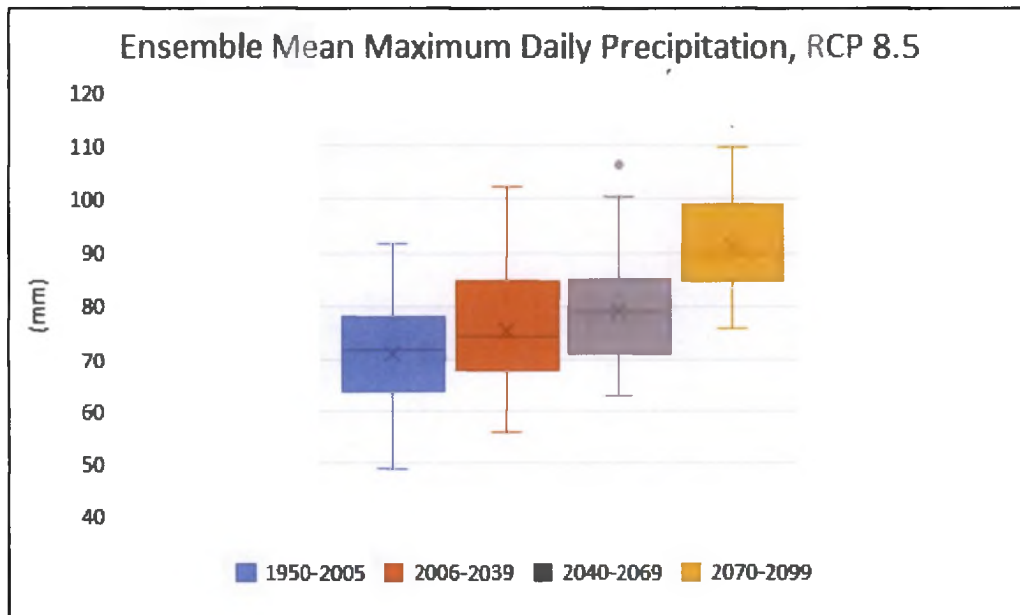
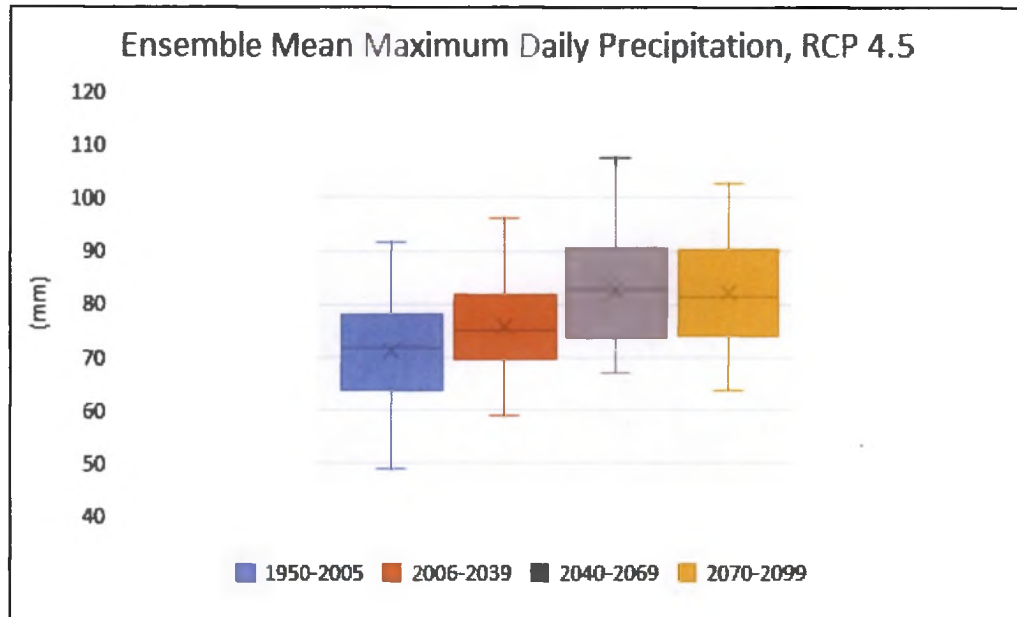


Figure 11: Change in annual maximum daily precipitation under RCP 4.5 and RCP 8.5. Box plots show range of 10-GCM ensemble means for each year of the indicated time periods.

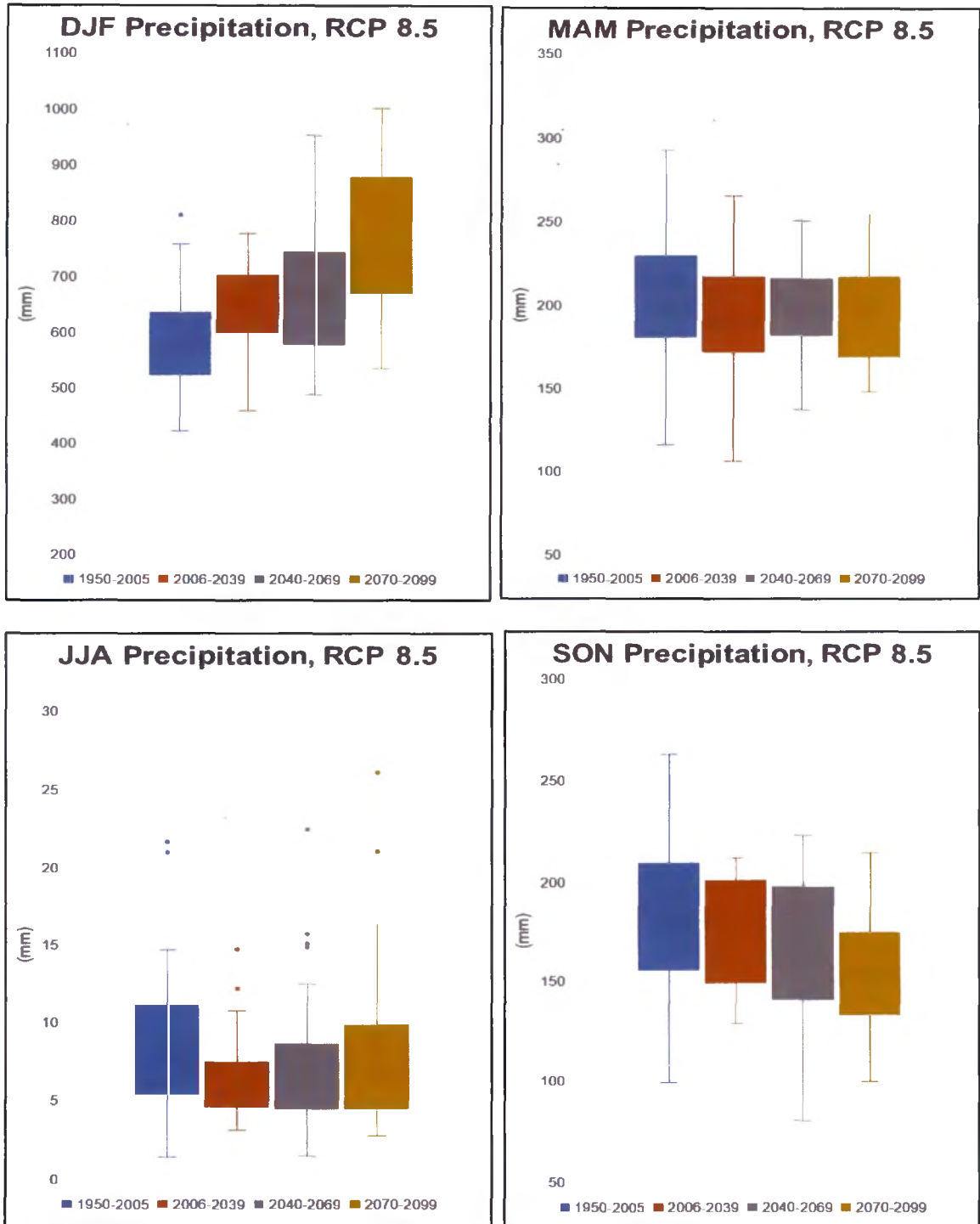


Figure 12: Changing distribution of total seasonal precipitation by time period for RCP 8.5 10-GCM ensemble mean. (DJF = winter, MAM = spring, JJA = summer, SON = fall).

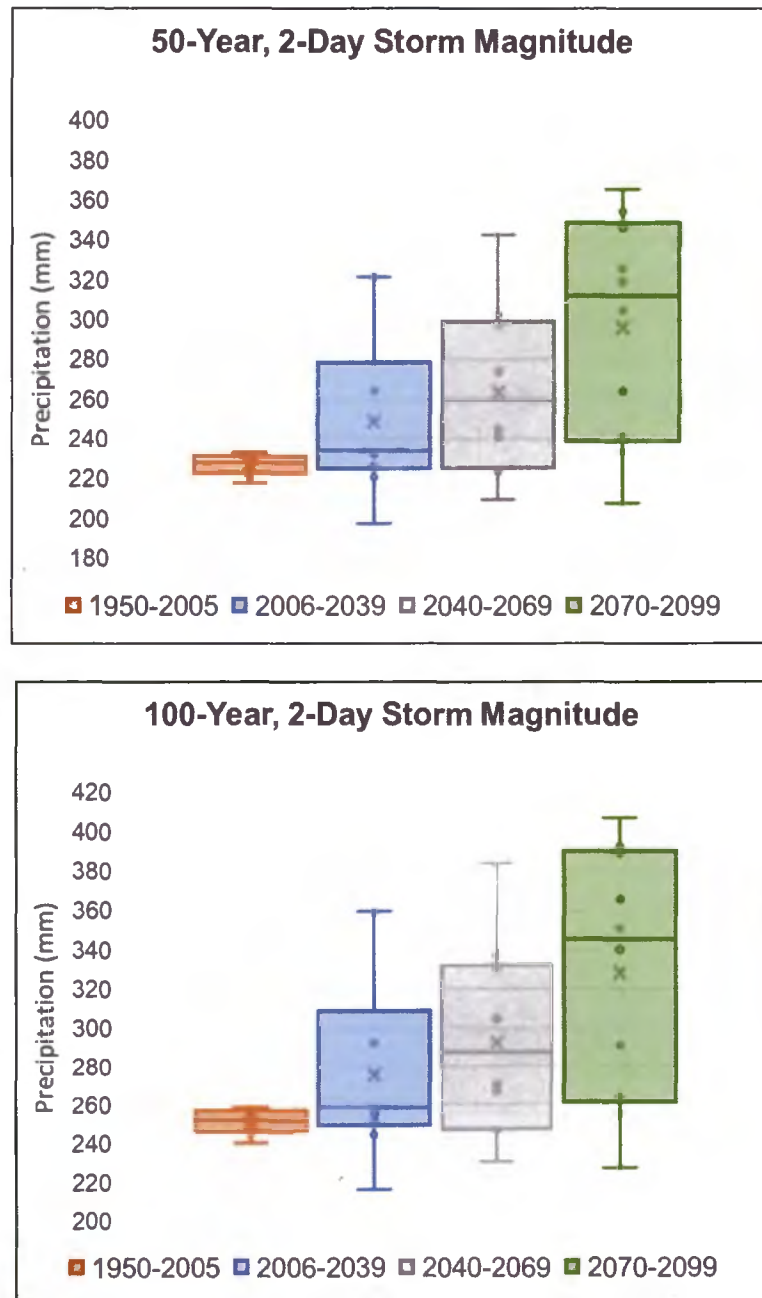


Figure 13: Changing distribution across 10 GCMs of projected two-day storm magnitude for 50-year and 100-year storms under RCP 8.5.

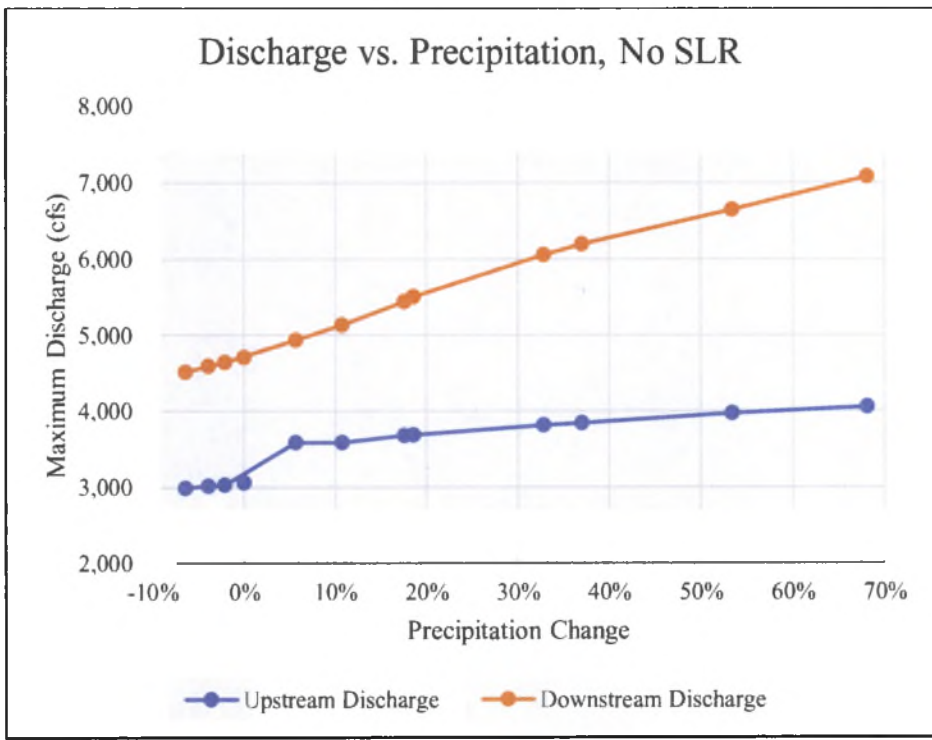


Figure 14: Modeled change in channel discharge as a function of change in precipitation magnitude for mid-century (2040-69) 50-year, 48-hour storm for each GCM (RCP 8.5). Upstream data corresponds to the location of the USGS Novato Creek stream gage. Downstream data corresponds to location of HEC-RAS model River Station (RS) 32080 as shown in Figure 4.

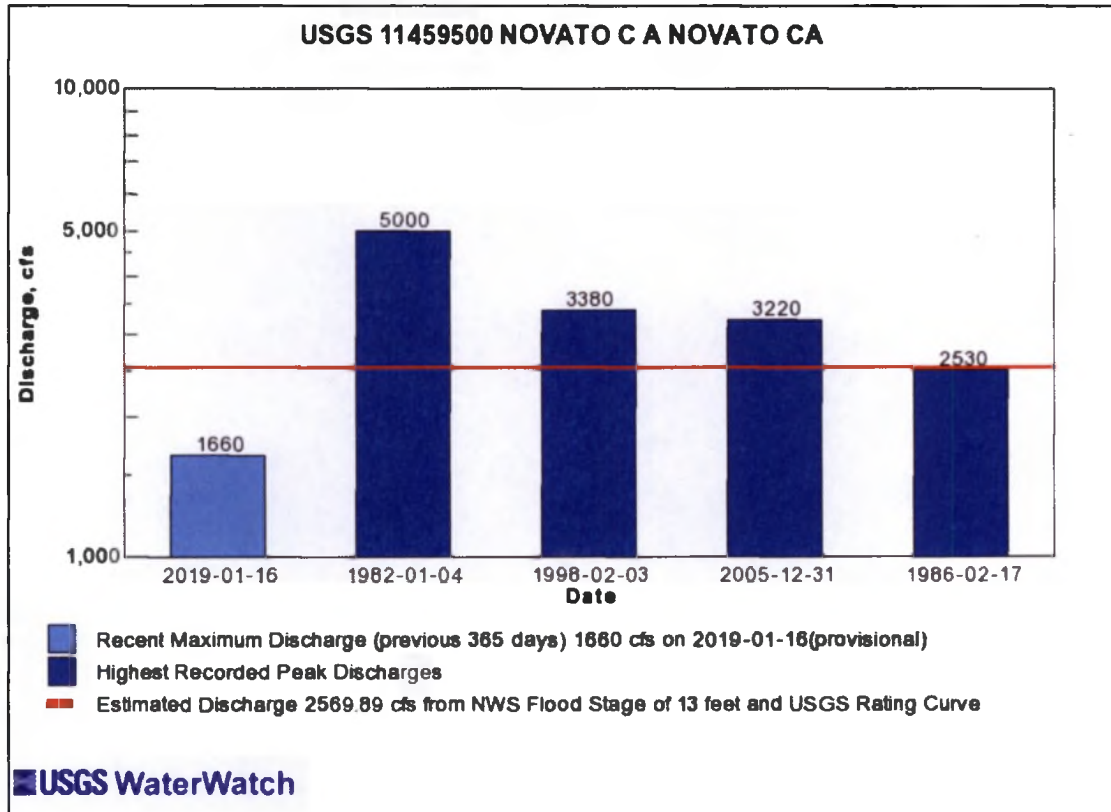


Figure 15: Novato Creek historic peak discharge and flood stage. Source: USGS Water Watch.

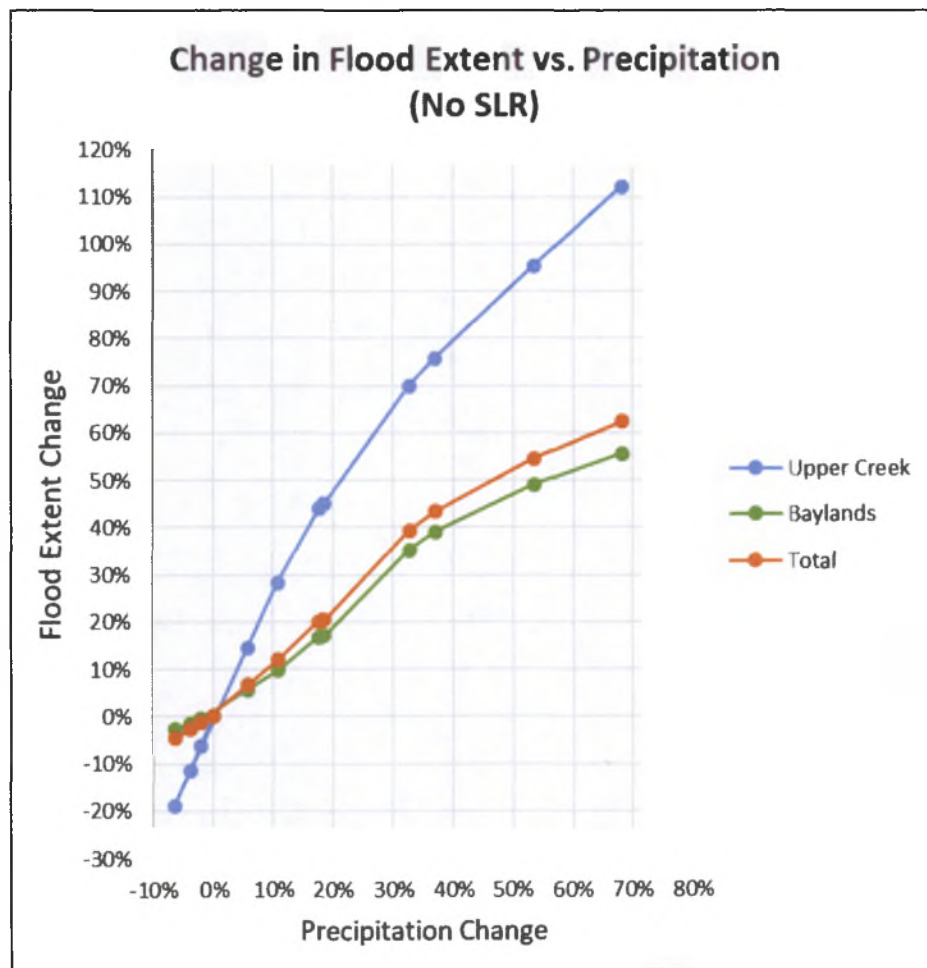


Figure 16: Change in flood extent as a function of change in precipitation magnitude for two-day, 50-year storm under RCP 8.5 with no SLR. Data points show all 10 GCM projections for mid-century, plus the maximum projection (CNRM-CM5) for late-century.

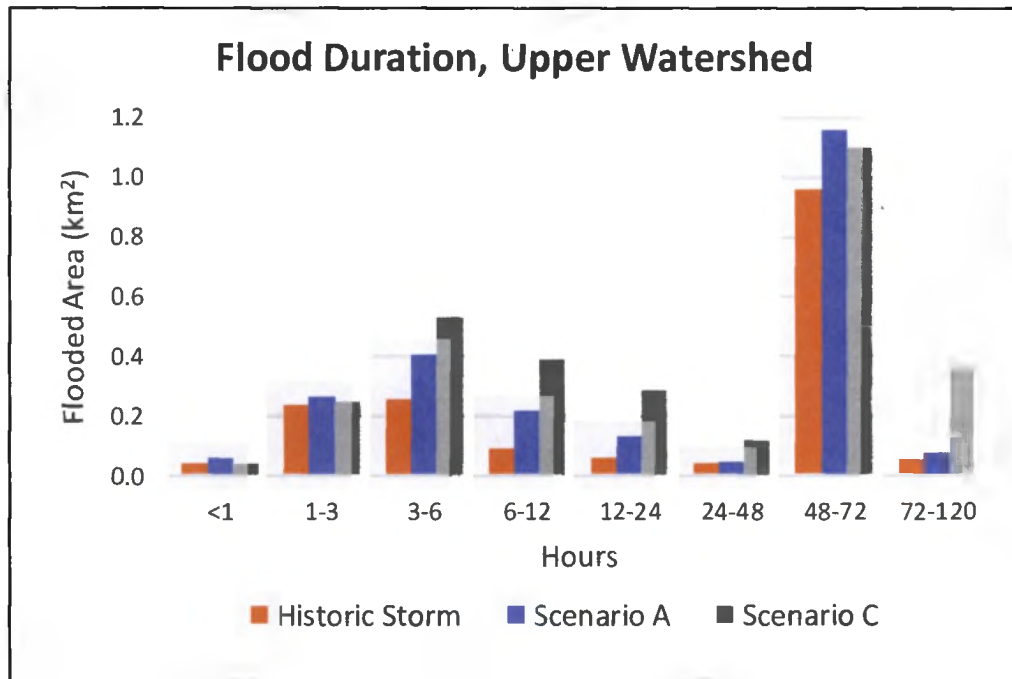


Figure 17: Flooded area in the Novato Creek upper watershed by duration of flooding, comparing the historic 50-year storm with mid-century and late-century compound flood scenarios.

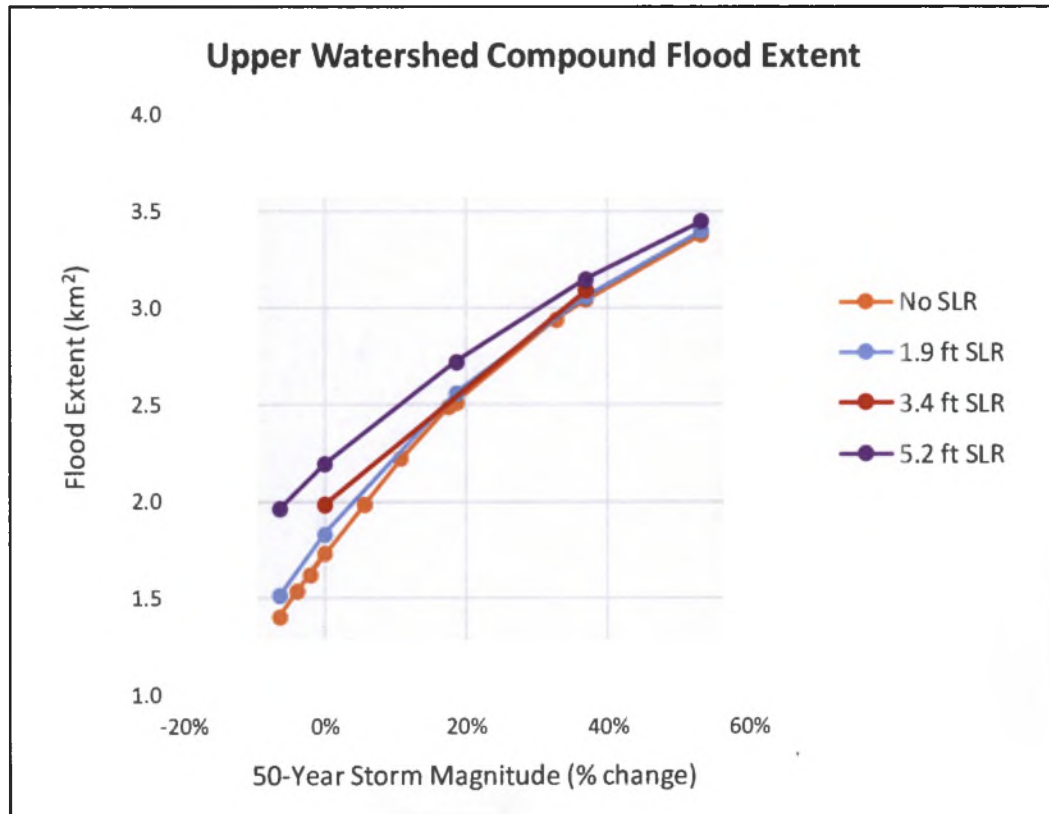


Figure 19: Modeled compound flood extent in the upper watershed only as a function of changes in 50-year storm magnitude under RCP 8.5 and different SLR.

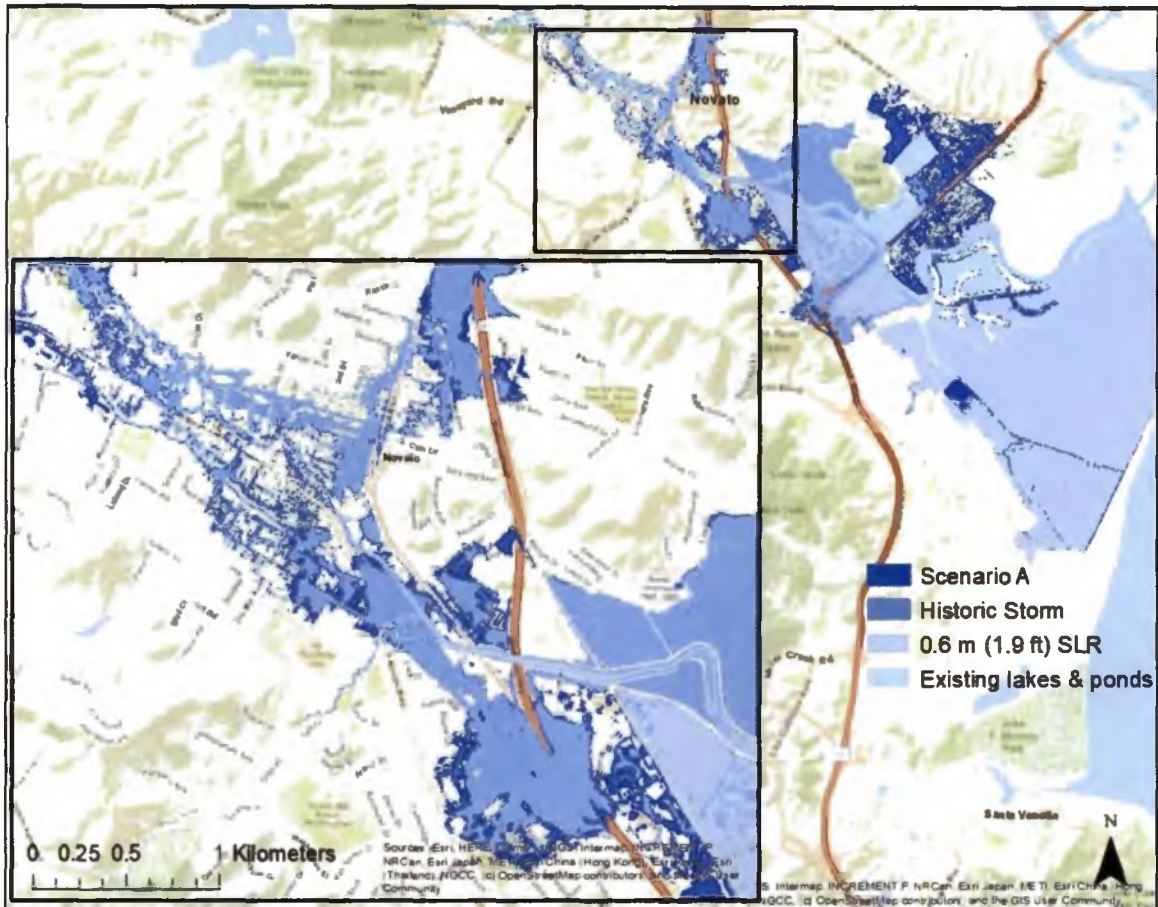


Figure 20: Comparison of Scenario A compound flood extent to area inundated by 0.6 m (1.9 ft) SLR and flood extent of historic 50-year storm. Inset shows closeup of downtown Novato and adjacent commercial and residential areas.

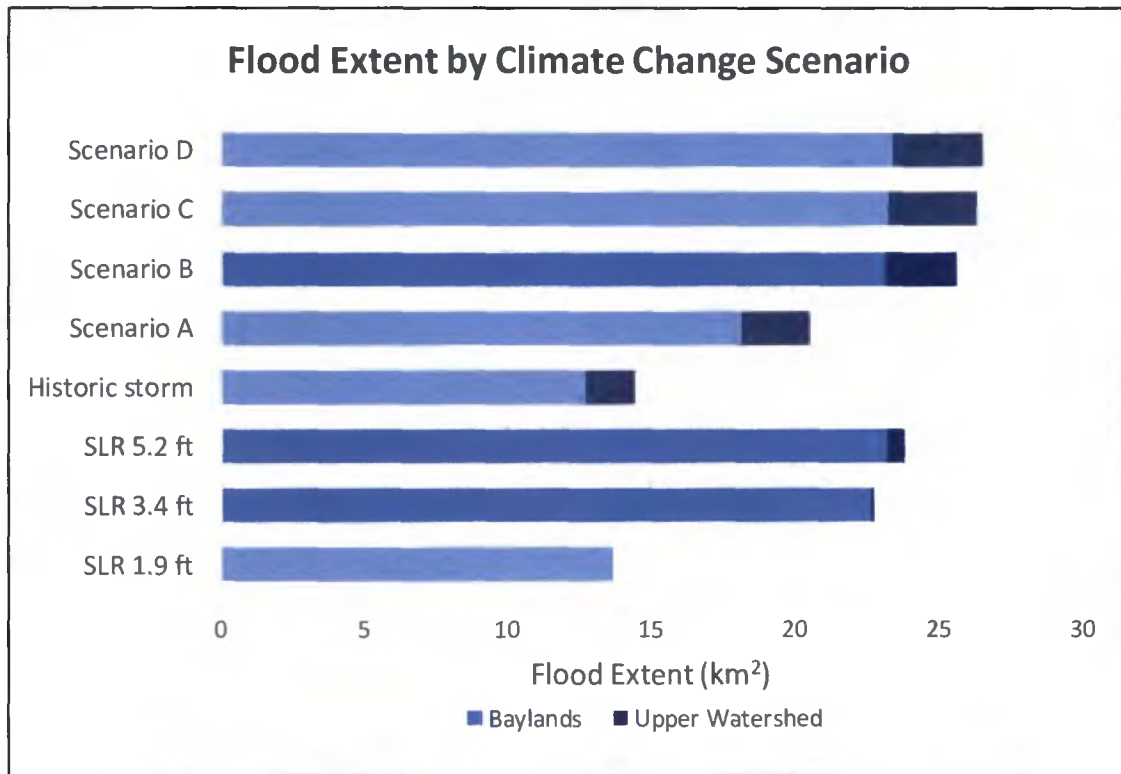


Figure 21: Flood extent by climate change scenario for two-day, 50-year storm. Scenarios A – D are described in Table 1.

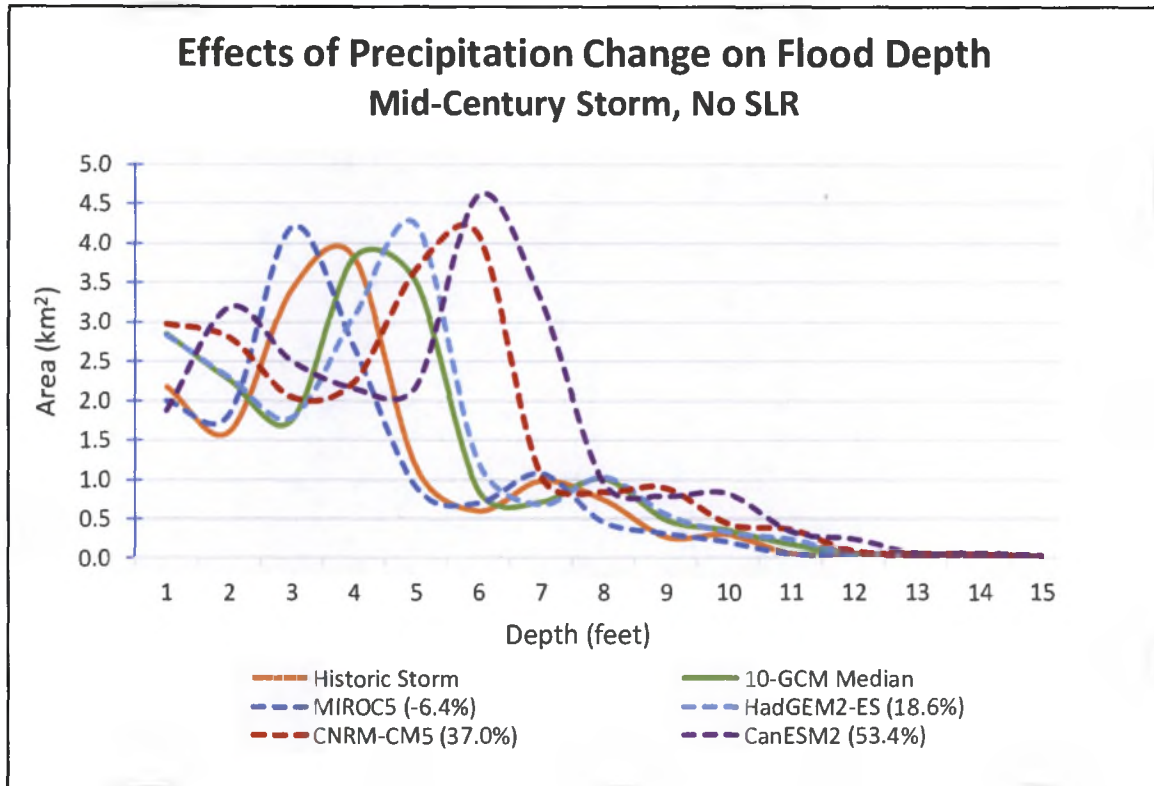


Figure 22: Distribution of flood depth by changing storm magnitude with no change in sea level. Results displayed are for the historic two-day, 50-year storm, mid-century projections for subset of four California GCMs, and mid-century 10-GCM ensemble median.

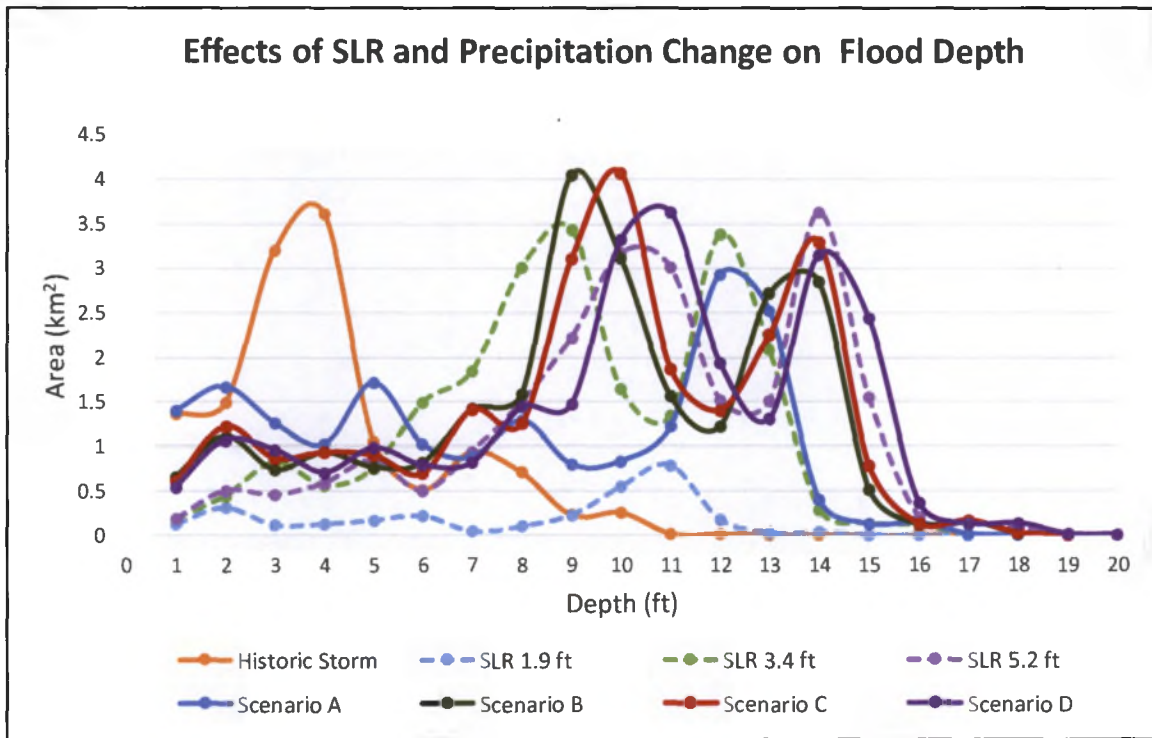


Figure 23: Comparison of effects of historic 50-year storm, SLR and compound climate change scenarios on distribution of flood depth.

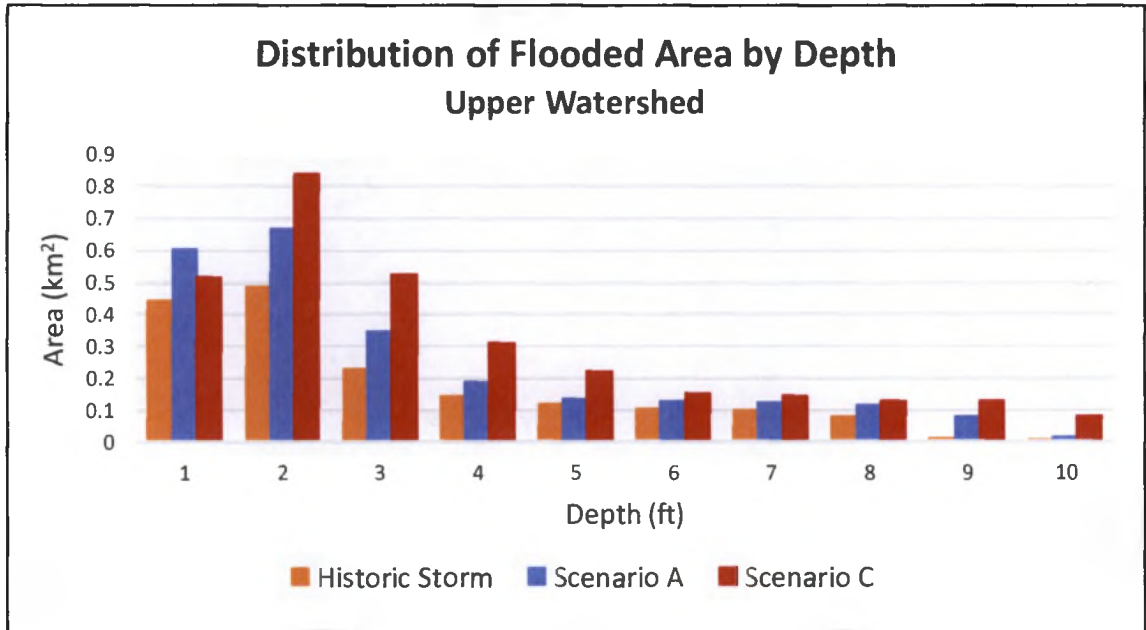


Figure 24: Distribution of flood depth by area flooded in the Novato Creek upper watershed, comparing the historic 50-year storm with mid-century and late-century compound flood scenarios.

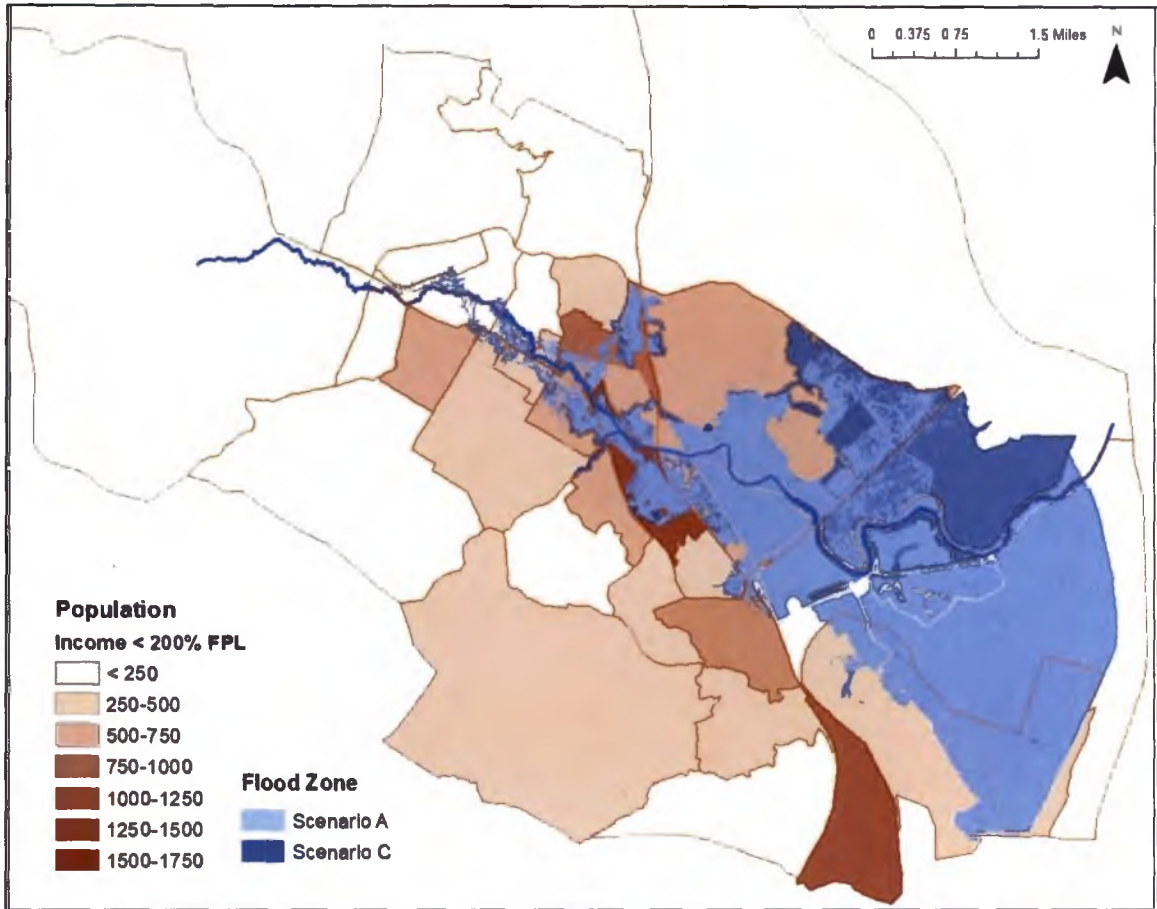


Figure 25: Distribution of low-income population by census block groups, relative to Scenario A (mid-century) and Scenario C (late-century) compound flood extent.

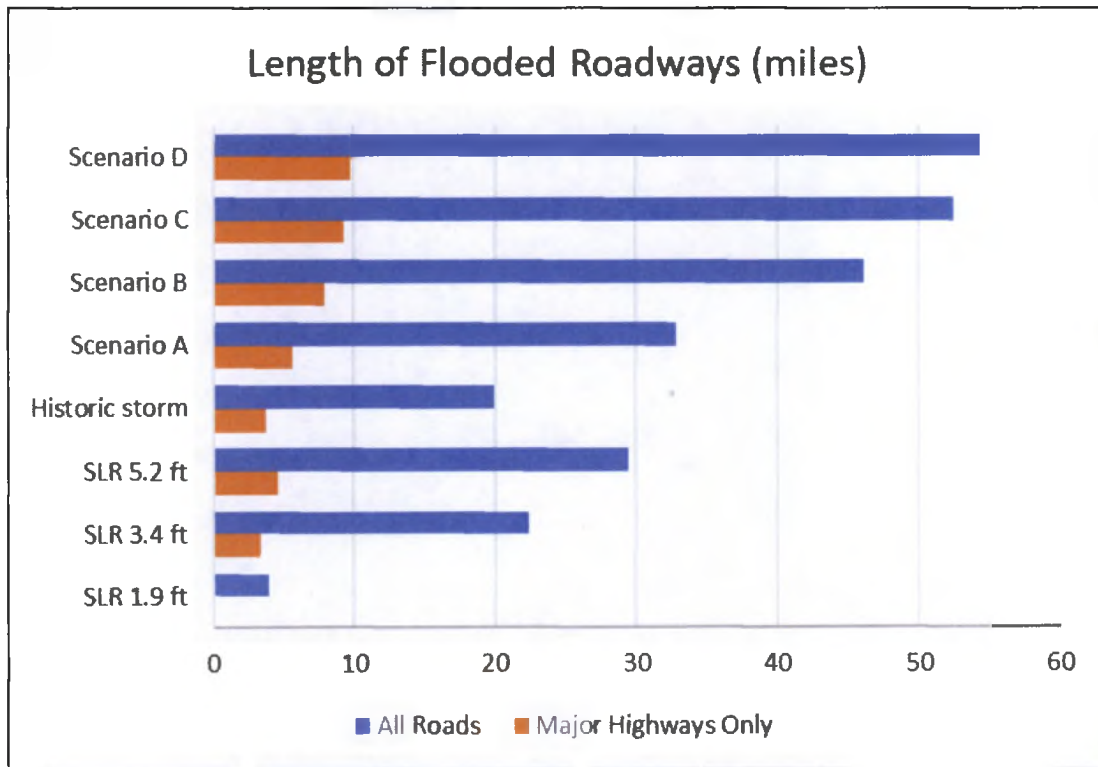


Figure 26: Length of flooded roadway showing changes under different scenarios for SLR and a 50-year, two-day storm under RCP 8.5.

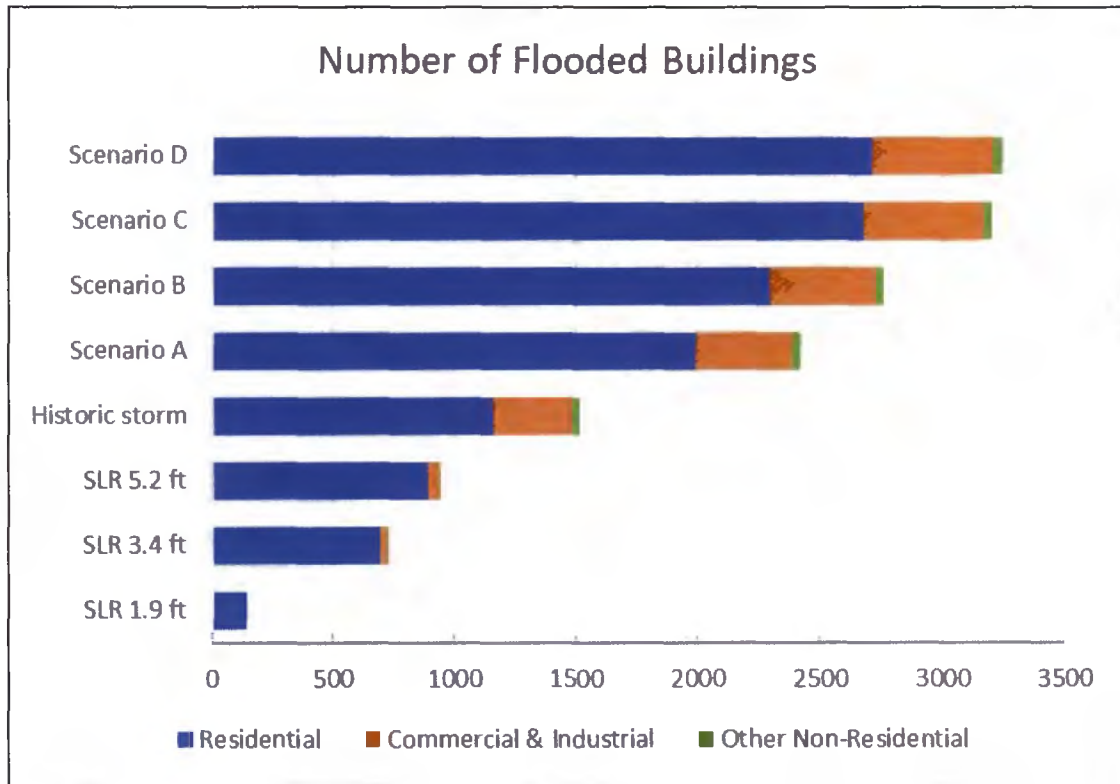


Figure 27: Number of inundated buildings by type of use, showing changes under different scenarios for SLR and a 50-year, two-day storm under RCP 8.5.

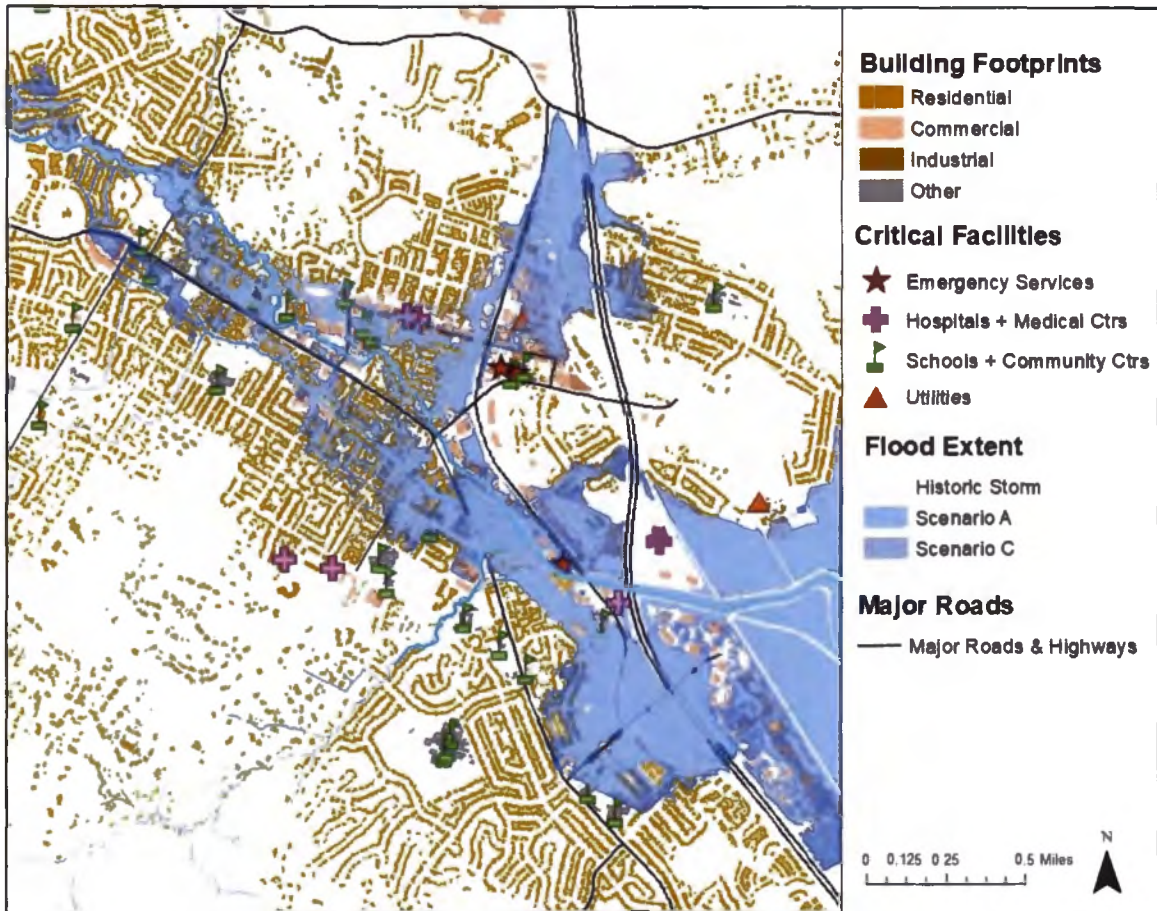


Figure 28: Map of Upper Novato Creek watershed showing location of buildings, critical facilities and major roads relative to flooding under historic 50-year storm and compound flood Scenarios A and C.

CMIP ACKNOWLEDGEMENT

I acknowledge the World Climate Research Programme's Working Group on Coupled Modelling, which is responsible for CMIP, and we thank the climate modeling groups (listed in Table 2 of this paper) for producing and making available their model output. For CMIP the U.S. Department of Energy's Program for Climate Model Diagnosis and Intercomparison provides coordinating support and led development of software infrastructure in partnership with the Global Organization for Earth System Science Portals.

REFERENCES

- Ackerly, D., Jones, A., Stacey, M., Riordan, B., 2018. San Francisco Bay Area Summary Report, California's Fourth Climate Change Assessment (No. CCCA4- SUM-2018- 005). University of California, Berkeley.
- Adger, W.N., 2006. Vulnerability. *Global Environmental Change* 16, 268–281. <https://doi.org/10.1016/j.gloenvcha.2006.02.006>
- AECOM, 2016. Extreme Storms in San Francisco Bay – Past to Present, Final Report. Federal Emergency Management Agency.
- Arnell, N.W., Gosling, S.N., 2016. The impacts of climate change on river flood risk at the global scale. *Climatic Change* 134, 387–401. <https://doi.org/10.1007/s10584-014-1084-5>
- Ballard, G., Barnard, P.L., Erikson, L., Fitzgibbon, M., Moody, D., Higgason, K., Psaros, M., Veloz, S., Wood, J., 2016. Our Coast Our Future (OCOF) [WWW Document]. URL www.ourcoastourfuture.org
- Barnard, P.L., Erikson, L.H., Foxgrover, A.C., Hart, J.A.F., Limber, P., O'Neill, A.C., Ormond, M. van, Vitousek, S., Wood, N., Hayden, M.K., Jones, J.M., 2019. Dynamic flood modeling essential to assess the coastal impacts of climate change. *Scientific Reports* 9, 4309. <https://doi.org/10.1038/s41598-019-40742-z>
- BCDC, 2017. Adapting to Rising Tides Bay Area Sea Level Rise Analysis and Mapping Project Final Report. San Francisco Bay Conservation and Development Commission.
- Blunden, J., Arndt, D.S., Hartfield, G. (Eds.), 2018. State of the Climate in 2017. *Bulletin of the American Meteorological Society* 99, 330. <https://doi.org/10.1175/2018>
- Brown, P.T., Caldeira, K., 2017. Greater future global warming inferred from Earth's recent energy budget. *Nature* 552, 45–50. <https://doi.org/10.1038/nature24672>
- BVB Consulting, 2017. Marin Shoreline Sea Level Rise Vulnerability Assessment, Bay Waterfront Adaptation & Vulnerability Evaluation (BayWAVE). Marin County Department of Public Works.
- Cayan, D.R., Bromirski, P.D., Hayhoe, K., Tyree, M., Dettinger, M.D., Flick, R.E., 2008. Climate change projections of sea level extremes along the California coast. *Climatic Change* 87, 57–73. <https://doi.org/10.1007/s10584-007-9376-7>

- Chen, W.-B., Liu, W.-C., 2014. Modeling Flood Inundation Induced by River Flow and Storm Surges over a River Basin. *Water*; Basel 6, 3182–3199. <http://dx.doi.org/jpllnet.sfsu.edu/10.3390/w6103182>
- Chen, Y., Moufouma-Okia, W., Masson-Delmotte, V., Zhai, P., Pirani, A., 2018. Recent Progress and Emerging Topics on Weather and Climate Extremes Since the Fifth Assessment Report of the Intergovernmental Panel on Climate Change. *Annual Review of Environment and Resources* 43, 35–59. <https://doi.org/10.1146/annurev-environ-102017-030052>
- Climate Central, 2019. Surging Seas Risk Finder [WWW Document]. Climate Central. URL <http://riskfinder.climatecentral.org>
- Couasnon, A., Sebastian, A., Morales-Nápoles, O., 2018. A Copula-Based Bayesian Network for Modeling Compound Flood Hazard from Riverine and Coastal Interactions at the Catchment Scale: An Application to the Houston Ship Channel, Texas. *Water* 10, 1190. <https://doi.org/10.3390/w10091190>
- Cutter, S.L., 2016. The landscape of disaster resilience indicators in the USA. *Nat Hazards* 80, 741–758. <https://doi.org/10.1007/s11069-015-1993-2>
- Cutter, S.L., Boruff, B.J., Shirley, W.L., 2003. Social Vulnerability to Environmental Hazards. *Social Science Quarterly* 84, 242–261. <https://doi.org/10.1111/1540-6237.8402002>
- Cutter, S.L., Emrich, C.T., 2017. Social Vulnerability Index (SoVI®): Methodology and Limitations.
- Dahl, K., Cleetus, R., Spanger-Siegfried, E., Udvardy, S., Caldas, A., Worth, P., 2018. Underwater: Rising Seas, Chronic Floods, and the Implications for US Coastal Real Estate. Union of Concerned Scientists.
- Dahl, K.A., Spanger-Siegfried, E., Caldas, A., Udvardy, S., 2017. Effective inundation of continental United States communities with 21st century sea level rise. *Elem Sci Anth* 5, 37. <https://doi.org/10.1525/elementa.234>
- Das, T., Maurer, E.P., Pierce, D.W., Dettinger, M.D., Cayan, D.R., 2013. Increases in flood magnitudes in California under warming climates. *Journal of Hydrology* 501, 101–110. <https://doi.org/10.1016/j.jhydrol.2013.07.042>
- Dettinger, M., 2011. Climate Change, Atmospheric Rivers, and Floods in California – A Multimodel Analysis of Storm Frequency and Magnitude Changes. *JAWRA Journal of the American Water Resources Association* 47, 514–523. <https://doi.org/10.1111/j.1752-1688.2011.00546.x>

- Dettinger, M., Anderson, J., Anderson, M., Brown, L.R., Cayan, D., Maurer, E., 2016. Climate Change and the Delta. *San Francisco Estuary and Watershed Science* 14.
- Downscaled CMIP3 and CMIP5 Climate and Hydrology Projections [WWW Document], 2016. URL https://gdo-dcp.ucllnl.org/downscaled_cmip_projections/ (accessed 12.15.17).
- DWR, 2015. Perspectives and Guidance for Climate Change Analysis. California Department of Water Resources, Climate Change Technical Advisory Group.
- Erikson, L.H., O'Neill, A.C., Barnard, P.L., 2018. Estimating Fluvial Discharges coincident with 21st Century Coastal Storms Modeled with CoSMoS. *Journal of Coastal Research* 791–795. <https://doi.org/10.2112/SI85-159.1>
- FEMA, 2009. Guidelines and Specifications for Flood Hazard Mapping Partners: Appendix C Guidance for Riverine Flooding Analyses and Mapping.
- Flanagan, B.E., Gregory, E.W., Hallisey, E.J., Heitgerd, J.L., Lewis, B., 2011. A Social Vulnerability Index for Disaster Management. *Journal of Homeland Security and Emergency Management* 8. <https://doi.org/10.2202/1547-7355.1792>
- Fothergill, A., Peek, L.A., 2004. Poverty and Disasters in the United States: A Review of Recent Sociological Findings. *Natural Hazards; Dordrecht* 32, 89–110. <http://dx.doi.org/jpllnet.sfsu.edu/10.1023/B:NHAZ.0000026792.76181.d9>
- Franco, G.F., Cayan, D.R., Pierce, D.W., Thorne, J.H., Westerling, A.L., Thorne, J.H., 2018. Cumulative Global CO2 Emissions and their Climate Impacts from Local through Regional Scales. California's Fourth Climate Change Assessment (No. CCCA4- EXT-2018– 007). California Energy Commission.
- Griggs, G., Árvai, J, Cayan, D, DeConto, R, Fox, J, Fricker, HA, Kopp, RE, Tebaldi, C, Whiteman, EA, 2017. Rising Seas in California: An Update on Sea-Level Rise Science, California Ocean Protection Council Science Advisory Team Working Group. California Ocean Science Trust.
- Hao, Z., Singh, V., Hao, F., Hao, Z., Singh, V.P., Hao, F., 2018. Compound Extremes in Hydroclimatology: A Review. *Water* 10, 718. <https://doi.org/10.3390/w10060718>
- Hino, M., Belanger, S.T., Field, C.B., Davies, A.R., Mach, K.J., 2019. High-tide flooding disrupts local economic activity. *Science Advances* 5, eaau2736. <https://doi.org/10.1126/sciadv.aau2736>
- Ikeuchi, H., Hirabayashi, Y., Yamazaki, D., Muis, S., Ward, P.J., Winsemius, H.C., Verlaan, M., Kanae, S., 2017. Compound simulation of fluvial floods and storm

- surges in a global coupled river-coast flood model: Model development and its application to 2007 Cyclone Sidr in Bangladesh. *Journal of Advances in Modeling Earth Systems* 9, 1847–1862. <https://doi.org/10.1002/2017MS000943>
- IPCC, 2013. Summary for Policymakers. In: *Climate Change 2013: The Physical Science Basis. Contribution of Working Group I to the Fifth Assessment Report of the Intergovernmental Panel on Climate Change*, in: Stocker, T.F., Qin, D., Plattner, G.K., Tignor, M., S.K. Allen, J. Boschung, A. Nauels, Y. Xia, V. Bex, P.M. Midgley (Eds.), . Cambridge University Press, Cambridge, United Kingdom and New York, NY.
- J. Lian, J., Xu, K., Ma, C., 2013. Joint impact of rainfall and tidal level on flood risk in a coastal city with a complex river network: a case study for Fuzhou city, China. *Hydrology and Earth System Sciences* 17, 679–689. <https://doi.org/DOI:10.5194/hess-17-679-2013>
- Jones, Jeanne, Wood, N., Ng, P., Henry, K., Jones, Jamie, Peters, J., Jamieson, M., 2016. Community Exposure in California to Coastal Flooding Hazards Enhanced by Climate Change, reference year 2010. <https://doi.org/10.5066/f7pz56zd>
- Kew, S.F., Selten, F.M., Lenderink, G., Hazeleger, W., 2013. The simultaneous occurrence of surge and discharge extremes for the Rhine delta. *Natural Hazards and Earth System Sciences* 13, 2017–2029. <https://doi.org/10.5194/nhess-13-2017-2013>
- KHE, 2014. Hydraulic Assessment of Existing Conditions: Novato Creek Watershed Project, Report to Marin County Department of Public Works. Kamman Hydrology & Engineering.
- Klerk, W.J., Winsemius, H.C., van Verseveld, W.J., Bakker, A.M.R., Diermanse, F.L.M., 2015. The co-occurrence of storm surges and extreme discharges within the Rhine–Meuse Delta. *Environmental Research Letters* 10, 035005. <https://doi.org/10.1088/1748-9326/10/3/035005>
- Kopp, R.E., DeConto, R.M., Bader, D.A., Hay, C.C., Horton, R.M., Kulp, S., Oppenheimer, M., Pollard, D., Strauss, B.H., 2017. Evolving Understanding of Antarctic Ice-Sheet Physics and Ambiguity in Probabilistic Sea-Level Projections. *Earth's Future* 5, 1217–1233. <https://doi.org/10.1002/2017EF000663>
- Kopp, R.E., Horton, R.M., Little, C.M., Mitrovica, J.X., Oppenheimer, M., Rasmussen, D.J., Strauss, B.H., Tebaldi, C., 2014. Probabilistic 21st and 22nd century sea-level projections at a global network of tide-gauge sites. *Earth's Future* 2, 383–406. <https://doi.org/10.1002/2014EF000239>

- Kumbier, K., Carvalho, R.C., Vafeidis, A.T., Woodroffe, C.D., 2018. Investigating compound flooding in an estuary using hydrodynamic modelling: A case study from the Shoalhaven River, Australia. *Natural Hazards and Earth System Sciences* 18, 463–477.
- Kundzewicz, Z.W., Kanae, S., Seneviratne, S.I., Handmer, J., Nicholls, N., Peduzzi, P., Mechler, R., Bouwer, L.M., Arnell, N., Mach, K., Muir-Wood, R., Brakenridge, G.R., Kron, W., Benito, G., Honda, Y., Takahashi, K., Sherstyukov, B., 2014. Flood risk and climate change: global and regional perspectives. *Hydrological Sciences Journal* 59, 1–28. <https://doi.org/10.1080/02626667.2013.857411>
- Leonard, M., Westra, S., Phatak, A., Lambert, M., van den Hurk, B., McInnes, K., Risbey, J., Schuster, S., Jakob, D., Stafford-Smith, M., 2014. A compound event framework for understanding extreme impacts. *WIREs: Climate Change* 5, 113–128. <https://doi.org/10.1002/wcc.252>
- Leventhal, R., 2013. Summary of HEC-HMS Hydrologic Analysis of the Novato Creek Watershed (Draft) (Technical Memorandum, Flood Control Watershed Group). Marin County Department of Public Works.
- Livneh, B., Bohn, T.J., Pierce, D.W., Munoz-Arriola, F., Nijssen, B., Vose, R., Cayan, D.R., Brekke, L., 2015. A spatially comprehensive, hydrometeorological data set for Mexico, the U.S., and Southern Canada 1950–2013. *Scientific Data* 2, 150042. <https://doi.org/10.1038/sdata.2015.42>
- Maurer, E.P., 2007. Uncertainty in hydrologic impacts of climate change in the Sierra Nevada, California, under two emissions scenarios. *Climatic Change* 82, 309–325. <https://doi.org/10.1007/s10584-006-9180-9>
- Maurer, E.P., Brekke, L., Pruitt, T., Thrasher, B., Long, J., Duffy, P., Dettinger, M., Cayan, D., Arnold, J., 2014. An Enhanced Archive Facilitating Climate Impacts and Adaptation Analysis. *Bulletin of the American Meteorological Society*, Boston 95, 1011–1019.
- Maurer, E.P., Kayser, G., Doyle, L., Wood, A.W., 2018. Adjusting Flood Peak Frequency Changes to Account for Climate Change Impacts in the Western United States. *Journal of Water Resources Planning and Management* 144, 05017025. [https://doi.org/10.1061/\(ASCE\)WR.1943-5452.0000903](https://doi.org/10.1061/(ASCE)WR.1943-5452.0000903)
- Moftakhari, H.R., AghaKouchak, A., Sanders, B.F., Feldman, D.L., Sweet, W., Matthew, R.A., Luke, A., 2015. Increased nuisance flooding along the coasts of the United States due to sea level rise: Past and future. *Geophysical Research Letters* 42, 9846–9852. <https://doi.org/10.1002/2015GL066072>

- Moftakhari, H.R., Salvadori, G., AghaKouchak, A., Sanders, B.F., Matthew, R.A., 2017. Compounding effects of sea level rise and fluvial flooding. *Proceedings of the National Academy of Sciences* 114, 9785–9790.
- Moss, R.H., Babiker, M., Brinkman, S., Calvo, E., Carter, T., Edmonds, J.A., Elgizouli, I., Emori, S., Lin, E., Hibbard, K., Jones, R., Kainuma, M., Kelleher, J., Lamarque, J.F., Manning, M., Matthews, B., Meehl, J., Meyer, L., Mitchell, J., Nakicenovic, N., O'Neill, B., Pichs, R., Riahi, K., Rose, S., Runci, P.J., Stouffer, R., VanVuuren, D., Weyant, J., Wilbanks, T., van Ypersele, J.P., Zurek, M., 2008. *Towards New Scenarios for Analysis of Emissions, Climate Change, Impacts, and Response Strategies* (No. PNNL-SA-63186). Intergovernmental Panel on Climate Change, Geneva, Switzerland.
- Mote, P., Brekke, L., Duffy, P.B., Maurer, E., 2011. Guidelines for constructing climate scenarios. *Eos, Transactions American Geophysical Union* 92, 257–258. <https://doi.org/10.1029/2011EO310001>
- Mueller, D., 2013. HEC-HMS Model Review, Memorandum to Roger Leventhal, Marin County Department of Public Works. WRECO.
- Nguyen, T.T.X., Bonetti, J., Rogers, K., Woodroffe, C.D., 2016. Indicator-based assessment of climate-change impacts on coasts: A review of concepts, methodological approaches and vulnerability indices. *Ocean & Coastal Management* 123, 18–43. <https://doi.org/10.1016/j.ocecoaman.2015.11.022>
- NOAA, 2018. Sea Level Rise Viewer [WWW Document]. URL <https://coast.noaa.gov/slr/#/layer/slr/> (accessed 11.9.18).
- Ntegeka, V., Baguis, P., Roulin, E., Willems, P., 2014. Developing tailored climate change scenarios for hydrological impact assessments. *Journal of Hydrology* 508, 307–321. <https://doi.org/10.1016/j.jhydrol.2013.11.001>
- NWS, 2015. Hydrologic Information Center - Flood Loss Data [WWW Document]. National Oceanic and Atmospheric Administration (NOAA), National Weather Service. URL <http://www.nws.noaa.gov/hic/> (accessed 10.23.17).
- Olbert, A.I., Comer, J., Nash, S., Hartnett, M., 2017. High-resolution multi-scale modelling of coastal flooding due to tides, storm surges and rivers inflows. A Cork City example. *Coastal Engineering* 121, 278–296. <https://doi.org/10.1016/j.coastaleng.2016.12.006>
- OPC, 2018. State of California Sea-Level Rise Guidance, 2018 Update. Ocean Protection Council, California Natural Resources Agency.

- Orton, P.M., Conticello, F.R., Cioffi, F., Hall, T.M., Georgas, N., Lall, U., Blumberg, A.F., MacManus, K., 2018. Flood hazard assessment from storm tides, rain and sea level rise for a tidal river estuary. *Natural Hazards*. <https://doi.org/10.1007/s11069-018-3251-x>
- Pasquier, U., He, Y., Hooton, S., Goulden, M., Hiscock, K.M., 2018. An integrated 1D–2D hydraulic modelling approach to assess the sensitivity of a coastal region to compound flooding hazard under climate change. *Natural Hazards*. <https://doi.org/10.1007/s11069-018-3462-1>
- Perica, S., Dietz, S., Heim, S., Hiner, L., Maitaria, K., Martin, D., Pavlovic, S., Roy, I., Trypaluk, C., Unruh, D., Yan, F., Yekta, M., Zhao, T., Bonnin, G., Brewer, D., Chen, L.-C., Parzybok, T., Yarchoan, J., 2014. NOAA Atlas 14 Precipitation-Frequency Atlas of the United States Volume 6 Version 2.3: California. U.S. Department of Commerce, National Oceanic and Atmospheric Administration, National Weather Service, Silver Spring, Maryland.
- Petroliagkis, T.I., Voukouvalas, E., Disperati, J., Bidlot, J., 2016. Joint Probabilities of Storm Surge, Significant Wave Height and River Discharge Components of Coastal Flooding Events (No. EUR 27824 EN). European Commission, Joint Research Centre, Luxembourg.
- Pierce, D.W., Barnett, T.P., Santer, B.D., Gleckler, P.J., 2009. Selecting global climate models for regional climate change studies. *PNAS* 106, 8441–8446. <https://doi.org/10.1073/pnas.0900094106>
- Pierce, D.W., Cayan, D.R., Maurer, E.P., Abatzoglou, J.T., Hegewisch, K.C., 2015. Improved bias correction techniques for hydrological simulations of climate change. *Journal of Hydrometeorology* 16, 2421–2442.
- Pierce, D.W., Cayan, D.R., Thrasher, B.L., 2014. Statistical downscaling using localized constructed analogs (LOCA). *Journal of Hydrometeorology* 15, 2558–2585.
- Pierce, D.W., Das, T., Cayan, D.R., Maurer, E.P., Miller, N.L., Bao, Y., Kanamitsu, M., Yoshimura, K., Snyder, M.A., Sloan, L.C., Franco, G., Tyree, M., 2013. Probabilistic estimates of future changes in California temperature and precipitation using statistical and dynamical downscaling. *Climate Dynamics* 40, 839–856. <https://doi.org/10.1007/s00382-012-1337-9>
- Pierce, D.W., Kalansky, J.F., Cayan, D.R., 2018. Climate, Drought, and Sea Level Rise Scenarios for California’s Fourth Climate Change Assessment. (Scripps Institution of Oceanography), California Energy Commission.

- Russo, T.A., Fisher, A.T., Winslow, D.M., 2013. Regional and local increases in storm intensity in the San Francisco Bay Area, USA, between 1890 and 2010. *Journal of Geophysical Research: Atmospheres* 118, 3392–3401. <https://doi.org/10.1002/jgrd.50225>
- Schaaf & Wheeler, 2018a. Final Novato Creek Hydraulic Model Revisions Incorporating Review Comments from Stetson Engineers, Charles D. Anderson and Melissa E. Reardon Memorandum to Roger Leventhal, Marin County Department of Public Works, August 10, 2018.
- Schaaf & Wheeler, 2018b. Existing Condition Novato Creek HEC-RAS Model Documentation, Charles D. Anderson Memorandum to Roger Leventhal, Marin County Department of Public Works, July 2, 2018.
- Schaaf & Wheeler, 2018c. Existing Condition Novato Creek HEC-RAS Model Documentation, Charles D. Anderson Memorandum to Roger Leventhal, Marin County Department of Public Works, April 11, 2018.
- Schaaf & Wheeler, 2017. Final Report North Deer Island Flood Diversion Weir and Detention Basin and Novato Creek Corridor Widening Restoration Projects.
- Strauss, B., Tebaldi, C., Kulp, S., Cutter, S., Emrich, C., Rizza, D., Yawitz, D., 2014. California, Oregon, Washington and the Surging Sea: A vulnerability assessment with projections for sea level rise and coastal flood risk. Climate Central.
- Strauss, B., Tebaldi, C., Ziemiński, R., 2012. Facts and findings: Sea level rise and storm surge threats for California, Surging Seas. Climate Central.
- Swain, D.L., Langenbrunner, B., Neelin, J.D., Hall, A., 2018. Increasing precipitation volatility in twenty-first-century California. *Nature Climate Change* 8, 427–433. <https://doi.org/10.1038/s41558-018-0140-y>
- Sweet, W.V., Kopp, R.E., Weaver, C.P., Obeysekera, J., Horton, R.M., Thieler, E.R., Zervas, C., 2017. Global and Regional Sea Level Rise Scenarios for the United States, NOAA Technical Report. NOAA.
- Taylor, K.E., Stouffer, R.J., Meehl, G.A., 2011. An Overview of CMIP5 and the Experiment Design. *Bull. Amer. Meteor. Soc.* 93, 485–498. <https://doi.org/10.1175/BAMS-D-11-00094.1>
- Tebaldi, C., Strauss, B.H., Zervas, C.E., 2012. Modelling sea level rise impacts on storm surges along US coasts. *Environ. Res. Lett.* 7, 014032. <https://doi.org/10.1088/1748-9326/7/1/014032>

- Thomas, K., Hardy, R.D., Lazrus, H., Mendez, M., Orlove, B., Rivera-Collazo, I., Roberts, J.T., Rockman, M., Warner, B.P., Winthrop, R., 2019. Explaining differential vulnerability to climate change: A social science review. *Wiley Interdisciplinary Reviews: Climate Change* 10, e565. <https://doi.org/10.1002/wcc.565>
- UNISDR, 2015. *The Human Cost of Weather-Related Disasters 1995-2015*. UN Office for Disaster Risk Reduction.
- U.S. Census Bureau, 2019. 2012-2016 American Community Survey 5-Year Estimates [WWW Document]. American FactFinder. URL <https://factfinder.census.gov> (accessed 5.1.19).
- USACOE, 2016a. *Hydrologic Modeling System HEC-HMS User's Manual*. U.S. Army Corps of Engineers Institute for Water Resources Hydrologic Engineering Center (CEIWR-HEC).
- USACOE, 2016b. *HEC-RAS River Analysis System*. U.S. Army Corps of Engineers Institute for Water Resources Hydrologic Engineering Center.
- USGCRP, 2017. *Climate Science Special Report: Fourth National Climate Assessment, Volume I*, in: D.J., W., Fahey, D.W., Hibbard, K.A., Dokken, D.J., Stewart, B.C., Maycock, T.K. (Eds.), . U.S. Global Change Research Program, Washington, DC, USA, p. 470 pp.
- van den Hurk, B., van Meijgaard, E., de Valk, P., van Heeringen, K.-J., Gooijer, J., 2015. Analysis of a compounding surge and precipitation event in the Netherlands. *Environmental Research Letters* 10, 035001. <https://doi.org/10.1088/1748-9326/10/3/035001>
- Wahl, T., Jain, S., Bender, J., Meyers, S.D., Luther, M.E., 2015. Increasing risk of compound flooding from storm surge and rainfall for major US cities. *Nature Climate Change; London* 5, 1093–1097. <http://dx.doi.org/jpllnet.sfsu.edu/10.1038/nclimate2736>
- Ward, P.J., Couasnon, A., Eilander, D., Haigh, I.D., Hendry, A., Muis, S., Veldkamp, T.I.E., Winsemius, H.C., Wahl, T., 2018. Dependence between high sea-level and high river discharge increases flood hazard in global deltas and estuaries. *Environmental Research Letters* 13, 084012. <https://doi.org/10.1088/1748-9326/aad400>

- Warner, M.D., Mass, C.F., Salathé, E.P., 2014. Changes in Winter Atmospheric Rivers along the North American West Coast in CMIP5 Climate Models. *J. Hydrometeor.* 16, 118–128. <https://doi.org/10.1175/JHM-D-14-0080.1>
- Webster, T., McGuigan, K., Collins, K., MacDonald, C., 2014. Integrated River and Coastal Hydrodynamic Flood Risk Mapping of the LaHave River Estuary and Town of Bridgewater, Nova Scotia, Canada. *Water* 6, 517–546. <https://doi.org/10.3390/w6030517>
- Wein, A., Ratliff, J., Báez, A., Sleeter, R., 2016. Regional Analysis of Social Characteristics for Evacuation Resource Planning: ARkStorm Scenario. *Natural Hazards Review* 17, A4014002. [https://doi.org/10.1061/\(ASCE\)NH.1527-6996.0000161](https://doi.org/10.1061/(ASCE)NH.1527-6996.0000161)
- Willems, P., Vrac, M., 2011. Statistical precipitation downscaling for small-scale hydrological impact investigations of climate change. *Journal of Hydrology* 402, 193–205. <https://doi.org/10.1016/j.jhydrol.2011.02.030>
- Zheng, F., Westra, S., Leonard, M., Sisson, S.A., 2014. Modeling dependence between extreme rainfall and storm surge to estimate coastal flooding risk. *Water Resources Research* 50, 2050–2071. <https://doi.org/10.1002/2013WR014616>
- Zscheischler, J., Westra, S., Hurk, B., Seneviratne, S., Ward, P., Pitman, A., AghaKouchak, A., Bresch, D., Leonard, M., Wahl, T., Zhang, X., 2018. Future climate risk from compound events. *Nature Climate Change*. <https://doi.org/10.1038/s41558-018-0156-3>